Global continental and marine detrital ϵNd: An updated compilation for use in understanding marine Nd cycling

Suzanne Robinson, Ruza Ivanovic, Tina van de Flierdt, Cécile Blanchet, Tachikawa Kazuyo, Ellen Martin, Carys Cook, Trevor Williams, Lauren Gregoire, Yves Plancherel, et al.

Chemical Geology 567 (2021) 120119

Contents lists available at ScienceDirect

Chemical Geology

journal homepage: www.elsevier.com/locate/chemgeo

Global continental and marine detrital ε_{Nd}: An updated compilation for use in understanding marine Nd cycling

Suzanne Robinson [a,*], Ruza Ivanovic [a], Tina van de Flierdt [b], Cécile L. Blanchet [c], Kazuyo Tachikawa [d], Ellen E. Martin [e], Carys P. Cook (Falco)[e], Trevor Williams [f], Lauren Gregoire [a], Yves Plancherel [b], Catherine Jeandel [g], Thomas Arsouze [h]

[a] School of Earth and Environment, University of Leeds, Leeds LS2 9JT, UK
[b] Imperial College London, Department of Earth Science and Engineering, South Kensington Campus, Exhibition Road, London SW7 2AZ, UK
[c] GFZ German Research Centre for Geosciences, Climate Dynamics and Landscape Evolution, 14473 Potsdam, Germany
[d] Aix Marseille Univ, CNRS, IRD, INRAE, Coll France, CEREGE, Aix-en-Provence, France
[e] University of Florida, Department of Geological Sciences, Williamson Hall, Gainesville, FL 32611, United States
[f] Texas A&M University, 1000 Discovery Drive, College Station, TX 77845-9547, United States
[g] Laboratoire d'Etudes en Géophysique et Océanographie Spatiale (LEGOS, Université de Toulouse/CNRS/CNES/IRD/Université Paul Sabatier), Observatoire Midi-Pyrénées, 14 Avenue Edouard Belin, 31400 Toulouse, France
[h] Supercomputing Center-Centro Nacional de Supercomputación (BSC-CNS), Carrer de Jordi Girona, 29, 31, 08034 Barcelona, Spain

ARTICLE INFO

Editor: Dr. Karen Johannesson

Keywords:
Nd isotope composition
Oceanic margins
Sea floor
Database
Benthic flux
GEOTRACES

ABSTRACT

Understanding the role of sediment-water interactions in the oceanic cycling of neodymium (Nd) isotopes is essential for its reliable use as a modern and palaeoceanographic tracer of ocean circulation. However, the exact processes that control Nd cycling in the ocean are poorly defined and require an up-to-date knowledge of the sources, sinks and transformation of this tracer to and within the ocean (e.g. as per the GEOTRACES core mission). We propose a considerable improvement of Nd-source identification by providing an extensive and up-to-date compilation of published terrestrial and marine sedimentary Nd isotopic measurements. From this database, we construct high resolution, gridded, global maps that characterise the Nd-isotopic signature of the continental margins and seafloor sediment. Here, we present the database, interpolation methods, and final data products. Consistent with the previous studies that inform our compilation, our global results show unradiogenic detrital Nd isotopic values ($\varepsilon_{Nd} \approx$ -20) in the North Atlantic, ε_{Nd} values of $\approx$ -12 to -7 in the Indian and Southern Ocean, and radiogenic values ($\varepsilon_{Nd} \approx$ -3 to +4) in the Pacific. The new, high-resolution interpolation is useful for improving conceptual knowledge of Nd sources and sinks and enables the application of isotope-enabled ocean models to understand targeted Nd behaviour in the oceans. Such applications may include: examining the strength and distribution of a possible benthic flux required to reconcile global Nd budgets, establishing the potential use of Nd isotopes as a kinematic tracer of ocean circulation, and a general quantification of the non-conservative sedimentary processes that may contribute to marine Nd cycling.

1. Introduction/Background

The Nd isotope composition of seawater is typically expressed in the epsilon notation (ε_{Nd}), denoting the deviation of a sample's $^{143}Nd/^{144}Nd$ ratio from the chondritic uniform reservoir (CHUR) or bulk earth ratio of 0.512638 in parts per 10,000 (Jacobsen and Wasserburg, 1980):

$$\varepsilon_{Nd} = \left(\frac{\left(^{143}Nd/^{144}Nd\right)_{sample}}{\left(^{143}Nd/^{144}Nd\right)_{CHUR}} - 1 \right) \times 10^4 \quad (1)$$

ε_{Nd} varies with the age and composition of Earth's crust (Goldstein and Hemming, 2003), such that different regions have distinct ε_{Nd} signatures. Older continental crust generally has a more negative (i.e. 'unradiogenic') ε_{Nd} signature compared with younger mantle derived material, as demonstrated in the compilation by Jeandel et al. (2007).

* Corresponding author.
E-mail address: ee14s2r@leeds.ac.uk (S. Robinson).

https://doi.org/10.1016/j.chemgeo.2021.120119
Received 1 December 2020; Received in revised form 26 January 2021; Accepted 3 February 2021
Available online 11 February 2021

This spatial heterogeneity in crustal ε_{Nd} and the dominance of crustal sources of Nd to the ocean forms the foundation of the use of ε_{Nd} as a water provenance tracer. Neodymium has a shorter deep-ocean residence time than the typical global ocean mixing time (≈ 1500 years) (Arsouze et al., 2009; Goldstein and Hemming, 2003; Lynch-Stieglitz and Marchitto, 2003; Rempfer et al., 2011). As such, different water masses in the ocean are categorised by distinct ε_{Nd} that is derived from chemical weathering of the continents (Goldstein and Hemming, 2003; Lacan and Jeandel, 2005; Tachikawa et al., 2003). This isotopic signature is then redistributed via advection. Thus, water column ε_{Nd} measured in-situ for the present day or in sedimentary/seafloor archives for the past has been observed to track basin-scale ocean transports such as meridional overturning circulation (e.g. Basak et al., 2015; Dausmann et al., 2017; Howe et al., 2016; Hu and Piotrowski, 2018; Jonkers et al., 2015; Pöppelmeier et al., 2020a, 2020b; Roberts and Piotrowski, 2015; Wilson et al., 2015; Xie et al., 2014) and to reconstruct marine gateway events (Horikawa et al., 2010; Khélifi et al., 2014; Martin and Scher, 2006; Newkirk and Martin, 2009; Scher and Martin, 2006; Sepulchre et al., 2014; Stumpf et al., 2015; Stumpf et al., 2010). Such interpretations of ε_{Nd} rely on the assumption that in the absence of local lithogenic input, ε_{Nd} behaves conservatively.

Despite a general acceptance of the water mass tracer properties of ε_{Nd}, the usefulness of Nd isotopes as a proxy for ocean circulation is hampered by ambiguities in the modern cycling and oceanic budget of Nd, alongside a lack of constraints on the processes governing its marine distribution (Abbott et al., 2015a; Rempfer et al., 2011; Tachikawa et al., 2017). This has led to the ambiguous phrase of a 'quasi-conservative' tracer. Nonetheless, extensive progress has been made in understanding how different water masses acquire their ε_{Nd} (to give a few examples: Arsouze et al., 2009; Haley et al., 2017; Jeandel, 2016; Jeandel et al., 2013; Lacan et al., 2012; Rempfer et al., 2011; Siddall et al., 2008; Stichel et al., 2020; Tachikawa et al., 2017, Tachikawa et al., 2003; Flierdt et al., 2016; van de Flierdt et al., 2012; Wilson et al., 2013). It was initially thought that seawater labelling by lithogenic Nd inputs took place only at the surface via aeolian dust and dissolved riverine inputs (Bertram and Elderfield, 1993), and early modelling studies using the transport-matrix method with surface inputs did reproduce North Atlantic Nd distributions correctly/reliably based on these assumptions (Jones et al., 2008). However, considering surface inputs alone failed to balance both Nd concentration ([Nd]) and ε_{Nd} distributions globally, with authors highlighting that there must be a 'missing source' (i.e. missing global Nd flux into seawater; Arsouze et al., 2009; Jones et al., 2008; Rempfer et al., 2011; Siddall et al., 2008; Tachikawa et al., 2003). Furthermore, a partial decoupling of [Nd] and ε_{Nd} in seawater is observed, termed the 'Nd paradox' (Goldstein and Hemming, 2003). That is, while ε_{Nd} remains fairly constant, [Nd] becomes more concentrated with increasing depth in the water column, and very generally increases along the circulation pathway, overall being mostly lower in the North Atlantic and higher in the Pacific, displaying broadly what has been described as a 'nutrient-like behaviour' (Bertram and Elderfield, 1993; Flierdt et al., 2016). The current debate on the oceanic cycling of Nd is therefore centred around two related issues: (1) constraining the sources, sinks and internal cycling of Nd, and (2) the decoupled behaviour of [Nd] and ε_{Nd} ('Nd paradox').

Building on the initial understanding that Nd enters the ocean through continental weathering, an important role for particulates within marine biogeochemical cycling of Nd, especially particulate-seawater exchange occurring within marginal settings, has been observed, and proposed to account for imbalances in the global marine Nd budget and the 'Nd paradox'. This contribution from particulates to marine ε_{Nd} and [Nd] may be somewhat unsurprising since the global terrigenous particulate flux to the oceans exceeds the dissolved flux by a factor of 17-30, and as such, the particulate flux dominates fluvial transport of Nd to the oceans (Jeandel, 2016; Jeandel and Oelkers, 2015). Thus, dissolution of just a small proportion (1-3%) of this particulate material deposited annually into seawater can have a large impact on global marine Nd budgets and cycling (Jeandel and Oelkers, 2015). Chemical transfer reactions among terrestrially derived particles and seawater comprise of adsorption/desorption, ion exchange and dissolution/precipitation (Jeandel, 2016; Jeandel and Oelkers, 2015; Lacan and Jeandel, 2005; Tachikawa et al., 2003). While desorption and ion exchange are usually relatively rapid processes, driven by the relatively high pH and ionic strength of seawater compared to most river waters, dissolution and precipitation take longer (Jeandel and Oelkers, 2015; Rousseau et al., 2015). Dissolution therefore continues for as long as the minerals remain out of equilibrium with respect to the adjacent fluids, at rates that are commonly proportional to surface area (Jeandel and Oelkers, 2015).

A large proportion of this particle-seawater exchange is thought to occur predominantly within estuarine sediments and on continental margins (Rousseau et al., 2015). Chemical elements released from particle dissolution are available locally here as a result of proximity to lithogenic sources delivering dissolved and particulate material to the ocean, alongside high detrital and biogenic particle concentrations within the water column that act to promote rapid local reprecipitation as secondary phases due to seawater being close to saturated or supersaturated with respect to many mineral phases (Jeandel and Oelkers, 2015; Pearce et al., 2013). Such an exchange, termed 'boundary exchange' is capable of modifying the isotopic signature of a water mass without significantly affecting its concentration, and has been proposed as a major source of Nd into seawater (Arsouze et al., 2009; Jeandel et al., 2007; Rempfer et al., 2011; Tachikawa et al., 2017; Flierdt et al., 2016). Investigating this concept further, Arsouze et al. (2007) simulated a realistic global ε_{Nd} distribution using boundary exchange as the only source/sink term, demonstrating the potential for this process to be highly important for balancing the oceanic Nd cycle. Subsequent to this 2007 study, the release of Nd from dissolution of continental derived particulate material has been incorporated into global Nd modelling schemes (Arsouze et al., 2009; Gu et al., 2019; Rempfer et al., 2011), contributing 90-95% of the total simulated Nd flux to the ocean and thus providing a mechanism to account for the 'missing source'.

Another possible contributor to the 'Nd paradox' is reversible scavenging; the physical process of adsorption and desorption of Nd onto sinking particle surfaces in the water column, now considered another important feature of the interplay of particulate and dissolved Nd phases in the ocean (Jeandel et al., 1995; Siddall et al., 2008; Stichel et al., 2020; Tachikawa et al., 1999). Modelling studies show that the observed pattern of increasing [Nd] with depth can be reproduced by parameterising internal cycling using the reversible scavenging approach developed by Bacon and Anderson (1982) (Arsouze et al., 2009; Gu et al., 2019; Pöppelmeier et al., 2020b; Rempfer et al., 2011; Siddall et al., 2008). These models operate under a steady state assumption, meaning external fluxes from particles are balanced by dissolution and adsorption, which is partitioned according to an equilibrium scavenging coefficient (K_D; Siddall et al., 2008).

This interplay between dissolved and particulate phases is a key aspect of the biogeochemical cycling of Nd that has sparsely been explored. As a result, K_D values have mostly been derived from research looking into the relationship between adsorbed and desorbed ^{231}Pa and ^{230}Th (Chase et al., 2002; Henderson et al., 1999; Siddall et al., 2007;

Siddall et al., 2005). Stichel et al. (2020) presented the first regional Nd particle-seawater interaction study in the North Atlantic, here investigating whether particle-seawater exchange occurs beyond settings proximal to where seawater acquires a weathering signal (i.e., does particle-seawater exchange take place in open ocean regions with low particle concentrations?). Comparing the difference in ε_{Nd} between the dissolved and particulate phases along the North Atlantic Deep Water (NADW) flow path, they found that particles become fully equilibrated with ambient seawater in the open ocean and therefore are no longer considered to be particle reactive. However, deep waters that are in contact with the seafloor, where nearly half of the total Nd is present in the particle phase (in comparison to approximately 5% in the open ocean), may present an exception to this condition. Here, increasing [Nd] profiles contrast with the more general observance that particle-seawater exchange *is* primarily limited to locales close to weathering inputs. This deviation has been attributed to either the reduced deep-water scavenging potential of Nd (Stichel et al., 2020), which would allow dissolved [Nd] to accumulate, or, to a previously neglected benthic source of Nd (e.g. the mobilisation of a secondary pool of reactive Nd; Abbott et al., 2015b; Haley et al., 2017).

Thus, a current branch of literature on Nd-cycling now proposes a change from a 'top-down' paradigm of Nd cycling (governed by aeolian dust inputs; dissolved riverine fluxes; boundary exchange, a sediment flux constrained to the continental margins; and internal cycling through reversible scavenging) to incorporate a 'bottom-up' model, whereby benthic fluxes and a sedimentary source at depth exert a significant control over the distribution of seawater Nd (Haley et al., 2017). This alternative model specifically refers to a transfer of Nd from sediment pore water to seawater resulting from early diagenetic reactions, and may explain imbalances in the marine ε_{Nd} budget as well as observed decoupling between water mass provenance and Nd isotopes (Abbott, 2019; Abbott et al., 2016; Abbott et al., 2015b; Abbott et al., 2015a; Du et al., 2016; Haley et al., 2017). It was initially offered as an explanation for measurements taken on the north-western Pacific margins, where it was inferred that radiogenic pore water Nd was transferred to overlying shallow and intermediate waters, and has thenceforth been proposed to exert a primary control over deep ocean ε_{Nd} (Abbott et al., 2016; Abbott et al., 2015a, 2015b). In particular, a benthic flux provides a mechanism to explain the deep water ε_{Nd} alteration in the North Pacific in the absence of deep water formation, where circulation is sluggish, and the sediments contain a considerable amount of volcanic material susceptible to leaching (Pearce et al., 2013). Under this benthic flux framework, ε_{Nd} of a water mass becomes determined by a combination of the circulation pathway and also non-mixing processes such as a bottom-sediment source, the influence of which can be determined from the magnitude and ε_{Nd} of the sediment flux coupled with the integrated time of exposure to this flux (i.e. exposure time) (Abbott et al., 2015a). In this sense, if benthic exposure time and detrital sediment composition can be reasonably predicted, ε_{Nd} may provide additional constraints concerning ocean circulation kinematics (Abbott et al., 2015a; Du et al., 2020; Haley et al., 2017).

Since the 2015 north-western Pacific studies, observations of large additions of Nd to the ocean from deep sites have been made in the Angola Basin off the southwest coast of Africa (Rahlf et al., 2020; Zheng et al., 2016) and the Rockall Trough in the North Atlantic (Crocket et al., 2018). Furthermore, measurements from the Tasman Sea revealed a flux of similar magnitude to that inferred for the North Pacific, suggesting regions with dominantly calcareous sediment could also contribute a significant source of Nd (Abbott, 2019). This presented an interesting challenge for understanding Nd cycling, since carbonate contains relatively low [Nd] and therefore regions dominated by calcareous sediments were previously considered an unlikely contributor to the benthic flux.

However, the presence of volcanic materials and calcareous sediments at the ocean interface can be highly localised, meaning that any potential Nd inputs from these sources are not seafloor-wide. Clays, on the other hand, are more ubiquitously spread throughout the global ocean, meaning that clay mineral dissolution might facilitate a large, widespread sedimentary Nd source to the ocean. Abbott et al. (2019) evaluated potential sedimentary Rare Earth Element (REE) host phases and concluded a benthic control of REEs, including Nd, could be driven by clay minerals that have high reactivates and large surface areas. The authors suggest that distal, deep ocean sites with fine-grained sediments may have the largest fluxes, as opposed to previous views that most of the Nd sediment source is highly constrained to margins. Consequently, the benthic flux could be widely applicable across the global ocean, providing another possible origin for the 'missing' Nd source. This model, however, assumes that reactivity and exchange capacity of certain mineral phases is similar across the globe, an assumption that still requires careful testing.

It is apparent that there remains many outstanding questions regarding particle-seawater exchange of Nd, in part due to an incomplete understanding of how these elements fractionate during mineral dissolution and precipitation (Pearce et al., 2013). Firstly, particle-seawater interaction of Nd involves a combination of complex processes (release, removal and exchange) operating under various temporal scales and under specific environmental conditions, for example pH or oxic-anoxic conditions, transport and aging of sedimentary deposits (Wilson et al., 2013). Our understanding of these processes is further complicated by the fact that particulate material is comprised of numerous mineral phases, each with its own distinct dissolution rate and saturation state, and as such, each fraction tends to be incongruently released by particle dissolution (Pearce et al., 2013; Wilson et al., 2013). Additionally, it has been argued that because Nd is commonly present in less reactive minerals, it is likely released to seawater at a slower rate than most other elements, enabling the potential of sediments deposited for a long time in the deepest part of the ocean to be weathered (Abbott et al., 2019).

Notably, it remains unconfirmed and sometimes hotly debated whether or not a benthic flux does exert a strong control on oceanic Nd distributions and what conditions influence the rate of such a flux. Simulating Nd cycling in 3D ocean models has been shown to help contribute to this debate, quantitatively evaluating the importance of different components of Nd cycling (Arsouze et al., 2009; Arsouze et al., 2007; Gu et al., 2019; Jones et al., 2008; Pöppelmeier et al., 2020b; Rempfer et al., 2011; Siddall et al., 2008). The most sophisticated global Nd schemes to date are implemented within coupled atmosphere-ocean general circulation models (AOGCMs), with an explicit description of the oceanic sources and sinks (e.g. Arsouze et al., 2009; Gu et al., 2019; Pöppelmeier et al., 2020b; Rempfer et al., 2011). They are currently predominantly based upon a 'top-down' model of marine Nd cycling, with a sediment flux constrained to the continental margins. However, Pöppelmeier et al. (2020b) recently began numerical-modelling investigations of the benthic flux within global marine Nd cycling by updating the Nd-isotope enabled Bern3D model initially developed by Rempfer et al. (2011) to explicitly account for a seafloor-wide source of Nd. The refined implementation included dissolution of resuspended riverine material in estuaries (Rousseau et al., 2015), and the removal of

the depth limitation for the sediment source (i.e. adapting the model's representation of 'boundary exchange', previously restricted to the upper 3000 m of the ocean, to thus invoke a benthic flux). The results of this study were useful for demonstrating the potential importance of including a seafloor-wide input of Nd.

Moreover, it has been argued that the 'top-down' and 'bottom-up' views of Nd cycling are not independent of each other (Du et al., 2020; Haley et al., 2017). Both may be essential for understanding and balancing the global marine ε_{Nd} budget and solving the 'Nd-paradox'. Despite the still enigmatic nature of Nd cycling in the ocean, a consistent theme to emerge from the expanding body of literature has been increasing evidence of the importance of the sediment-water interface as a dominant control on the marine Nd cycle (Abbott et al., 2015b; Arsouze et al., 2009; Arsouze et al., 2007; Blaser et al., 2019; Haley et al., 2017; Rempfer et al., 2011; Tachikawa et al., 2017; Tachikawa et al., 2003; Flierdt et al., 2016; Vogt-Vincent et al., 2020). With more Nd delivered to the oceans in the particulate phase relative to the dissolved phase, and just a small fraction of particle dissolution being capable of governing marine ε_{Nd} and [Nd] distributions, the dissolution of terrigenous particulate material may be the dominant mechanism by which Nd is supplied to the oceans (Jeandel and Oelkers, 2015). Although this may complicate the use of ε_{Nd} as a tracer of ocean circulation, it suggests that global marine cycling of Nd can provide additional constraints as a tracer of continental weathering and climate (Abbott et al., 2019; Jeandel and Oelkers, 2015; Pearce et al., 2013). If terrigenous particle dissolution does dominate Nd [isotope] input to the ocean, ε_{Nd} variations in different water masses could, in some cases, be directly relatable to changes in *sediment* (as opposed to *water*) provenance and the weathering of locally derived material. However, to be able to quantify such effects, it is first necessary to improve our incomplete knowledge of how different particulate Nd phases from diverse sedimentary environments fractionate during mineral dissolution and precipitation.

In short, notwithstanding significant recent advances in the way we think about Nd sources and sinks, sediment-water interactions remain one of the least understood aspects of marine Nd cycling. The proliferation of Nd measurements, and our evolving knowledge of Nd cycling now present an opportunity to test new conceptual and numerical models that explicitly account for the benthic flux occurring across the whole seafloor. This could be used to answer, to a first order, the current key questions around marine Nd cycling. Including, but not limited to: constraining the magnitude and ε_{Nd} from sediment-water interaction, testing whether a 'bottom up' framework is consistent with the observed modern seawater ε_{Nd} and [Nd], assessing any overprinting effect a benthic flux may have on bottom waters, and evaluating the possibility that with a strong benthic flux ε_{Nd} could be exploited as a kinematic tracer of ocean circulation.

However, all of these investigations require a known global distribution of sedimentary ε_{Nd}. Numerical modelling studies in particular rely on a spatially-continuous definition of Nd signatures across the whole global sediment-water interface as a model input, essentially filling-in the gaps between disparate measurement sites in a geologically robust way. More than a decade ago, Jeandel et al. (2007) produced a seminal map of continental ε_{Nd}, which fulfilled exactly this purpose, summarising the global fingerprint of continental ε_{Nd} inputs to the ocean and enabling numerical schemes to implement a continental margin source. Here, we build on this formative work, taking the opportunity to incorporate a substantial amount of recently published ε_{Nd} measurements to update the extrapolated data product for the continental margins and extend it across the whole ocean floor. Our new continuous distributions of ε_{Nd} thus provides the detail needed to evaluate a global sediment source of Nd to the ocean, or for the user to apply their own regional constraints depending on water depth, sediment thickness/type etc. In this way, we hope to facilitate a more complete understanding of Nd marine cycling, specifically enabling a first-order examination of the benthic flux in numerical modelling schemes to determine whether a shift towards a 'bottom-up' framework is capable of representing global oceanic Nd distributions.

In the following section, we describe the methods used to characterise the ε_{Nd} signature of the global sediment-water interface, including the new data compilation, our approach to filtering ε_{Nd} measurements and the process for producing the spatially continuous gridded maps (Section 2). Next, we present our refined continuous ocean sediment ε_{Nd} distributions, including ε_{Nd} at the continental margin and across the sea floor (Section 3). We then provide our proposed combination of both datasets and include a discussion about the final boundary conditions, acknowledging the limitations in our approach, and propose the use of these gridded maps as a first step towards a deeper interrogation of the sources and sinks of oceanic Nd, including the possibility of a benthic flux (Section 4).

The final ε_{Nd} maps clearly highlight where there is a wealth and conversely a dearth of Nd measurements, and where those measurements may or may not be representative of the wider oceanographic setting, thereby providing a useful guide for future data acquisition efforts. Furthermore, our methods are reproducible, and we provide full documentation of the protocol to facilitate updating the distributions with new measurements. Thus, we contend that our proposed sediment ε_{Nd} maps form an important and much needed step towards improving the understanding and quantification of marine Nd cycling under evolving frameworks and in line with the aims of the international GEOTRACES program, enabling future modelling efforts to answer the many intriguing questions that remain.

2. Methods

2.1. Updated database and compilation of published ε_{Nd}

An extensive and updated (relative to Jeandel et al., 2007) database of ε_{Nd} values measured on both terrestrial and marine sediments was initially obtained from Blanchet (2019). This database was built incorporating published Nd values from an extensive literature review, external contributions and retrieval from the SedDB database and includes 1,529 observations. We then identified areas where known additional published data could be added to the database and where observational data was spatially limited, having the potential to impede/bias interpolation across the globe. Notably, we prioritised detailed publications with numerous observations taken around key regions of deep-water formation in the North Atlantic and addressing data scarcity, particularly in the Pacific, Indian and Southern Ocean.

Through co-author contribution and a collective community effort to put forward relevant published datasets, the initial database was expanded to reach a total of 5,107 data points, including 2,671 present day and Holocene rock, river and marine sediment observations, thus capturing a much greater level of spatial detail in the overall larger quantity of constituent data (Fig. 1 and Supplementary Table S1). This was achieved first from extensive literature review, adding relevant observations particularly covering the Southwest Atlantic, the Bering Sea, the Southern Ocean, and West Africa. We then added further detail in the Southern Ocean, focusing along the Antarctic coastline, notably in West Antarctica, the Antarctic Peninsula and surrounding the Ross Sea (Cook et al., 2013; Mikhalsky et al., 2013; Mikhalsky et al., 2006; Pierce et al., 2011; Roy et al., 2007; Simões Pereira et al., 2018; van de Flierdt et al., 2008; Walter et al., 2000). This Southern Ocean compilation also

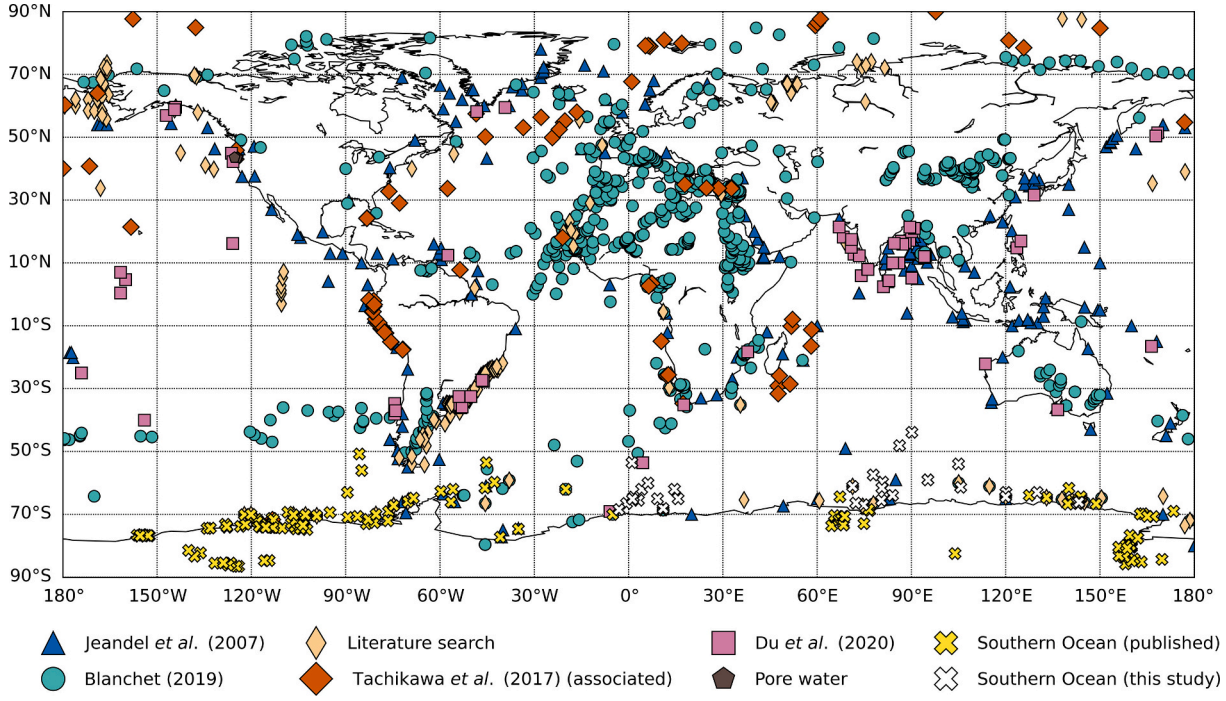

Fig. 1. Overview of the location of the ε_{Nd} samples assembled in the updated continental and marine detrital and porewater database, filtered to show only data from the Holocene (specifically 11.7 ka to present) and the new Southern Ocean data presented in this study. Data are identified as belonging to the initial sediment ε_{Nd} compilation by Jeandel et al. (2007) (blue triangles), subsequent additions by Blanchet (2019) (green circles), from further literature review (thin beige diamonds), detrital data associated with the results presented by Tachikawa et al. (2017) (orange diamonds), data compiled by Du et al. (2020) (lilac squares), pore water data from Abbott et al. (2015a, 2015b) (black pentagon) and Southern Ocean compilation (yellow crosses: published by Cook et al., 2013; Mikhalsky et al., 2013, Mikhalsky et al., 2006; Pierce et al., 2011; Roy et al., 2007; Simões Pereira et al., 2018; van de Flierdt et al., 2008; Walter et al., 2000. White crosses: this study).

includes a collection of 34 new (i.e. hitherto unpublished) measurements; see Supplementary Text S1 and Table S2 for information on the collection/measurement techniques. Our compilation of published and new Southern Ocean data is focussed on marine detrital measurements that could be used as an indicator of the ε_{Nd} signal eroded from neighbouring continental rock and also provides measurements from sediments directly in contact with seawater. We obtained even more modern and Holocene detrital measurements from sediments in the Arctic, eastern North Atlantic, West Atlantic, Gulf of Alaska and the Indian and East Pacific Ocean from the global compilation of detrital ε_{Nd} that accompanied the large-scale acquisition of seawater and geologic-archive ε_{Nd} performed by Tachikawa et al. (2017). Additionally, we include data from a recent global core-top compilation published by Du et al. (2020), whom investigated recent changes to Global Overturning Circulation from authigenic and sedimentary ε_{Nd} records, covering particularly the North-West and South-West Atlantic, the Indian and Central Equatorial Pacific Ocean. Finally, we included marine pore fluid ε_{Nd} from three sites in the eastern North Pacific (Abbott et al., 2015b; Abbott et al., 2015a).

The database, including the full dataset of ε_{Nd} and associated metadata table is reported in Supplementary Table S1 and the database will be stored on the GFZ data repository (see Data Availability).

2.2. Continental ε_{Nd} map

2.2.1. Data selection

The primary aim of this first phase of work is to define as accurately as possible the modern isotopic signatures of the continents surrounding the oceans and continental margins on a global scale. To achieve this aim, we filtered the entries in our new, comprehensive database (Section 2.1) to only include samples from the Holocene (specifically 11.7 ka to present) as well as the New Southern Ocean samples, which in some cases may be older, yet still provide appropriate ε_{Nd} for our study (as explained in Supplementary Text S1). We include present day (P) samples defined from 1 ka to present or from the upper 1cm/top-core sediment, and Holocene/Marine Isotope Stage 1 (MIS1) samples ranging from 11.7 – 1 ka. This is because we are most confident that the measured values falling within these depositional age ranges are representative of the modern continental ε_{Nd} interacting with seawater. This yielded a total of 1,078 observations, which came from three broad sample types: river sediment samples, which deposit on the continental shelf and slope; Holocene marine sediments collected along given margins; and geological material outcropping close to an oceanic margin expected to be weathered. We explain this choice in more detail in Supplementary Text S2. All the discrete continental data extracted through this filtering process are reported in Supplementary Table S3 and are displayed in Fig. 2a.

We acknowledge the potential for bottom ocean currents to transport fine-grained sediments to sites distal from their sources (Gorsline, 1984), and this may have a local/regional control on the ε_{Nd} passed on to the overlying water column (Jeandel et al., 2007). With currently available observations, this is difficult to consider comprehensively within a global, objective, numerically-driven framework. Thus, we assume that the effect of bottom-current transport is relatively small for the overall regional-global Nd budget and do not explicitly incorporate the process in our initial interpolation of the discrete data (Section 2.2.2). Future work that focuses on specific geographical domains would be best suited to investigating the importance and impact of these assumptions in greater detail.

2.2.2. *Interpolation of continental ε_{Nd} map*

Once an extensive compilation of suitable discrete ε_{Nd} observations was obtained, the points were interpolated across the globe, to create a spatially continuous distribution of continental ε_{Nd} proximal to the ocean. It is noted here that we are aiming to produce values that represent broader geological regions and not specific outcrops and singular observations.

Since the ε_{Nd} of continental rocks is closely related to its geological characteristics (i.e. lithology) and age, we used the digital geological map as used by Jeandel et al. (2007) – see 'Continental Geological Base Map' in Data Availability – which provided polygons for the (simplified) fields of given geological age and type. This map was used to constrain our interpolation of discrete data points according to the underlying geological units, maintaining a basic level of regional geological consistency in our continuous characterisation of the continental margins. Such an approach is based on the assumption that the seawater ε_{Nd} is equivalent to the ε_{Nd} signature of the weathered source rock, which we deem to be an appropriate premise for the global scale examined here.

The interpolation scheme employed a nearest neighbour analysis, using the digital geological map as a mask to produce spatially continuous continental ε_{Nd} fields from the discrete Nd point-measurements. Each geological-unit polygon was attributed an ε_{Nd} value according to the sample that fell within its spatial domain with the nearest distance to the centre of the polygon, or in the absence of any measurements within the domain, according to the nearest sample by distance to the centre of the polygon. This produced a first iteration of the new high resolution, gridded ε_{Nd} for continental margins (Supplementary Fig. S3) based purely on the numerical interpolation methods described above and without any expert 'tuning' of the results to account for any [sampling] biases that may skew the results. It forms the basis of our final continental margin ε_{Nd} distribution with the adaptations summarised below.

Examining this initial output, it is apparent that in some regions, the purely numerically based interpolation failed to capture the real spatial heterogeneity of crustal ε_{Nd}, or produced ε_{Nd} that, from our knowledge, appeared to not represent the broader regional signal, e.g. due to measurements capturing only very localised ε_{Nd} and the numerical interpolation inaccurately dispersing those signals. We therefore performed a small number of manual adjustments to the interpolation in order to improve the final distribution of ε_{Nd} and thus bring it into better accord with available evidence (i.e. the wider published literature) and the expert judgment and field/laboratory-experience of our pool of co-authors.

To assess the interpolation and identify where adjustments were needed, we closely interrogated the agreement between the numerically-produced ε_{Nd} and expected (e.g. based on geological age and rock type) ε_{Nd} within geological polygons based on the Sm-Nd evolution of Earth (i.e. age) and Sm/Nd fractionation during mantle melting (i.e. lithology; Goldstein et al., 1984; Taylor et al., 1983). In addition, we compared the signature of similar geographically distal fields (e.g. the same rock type/age, and regions that are known to have once been physically connected before tectonic plate movement separated them). Overall, we made the fewest possible changes to rectify obtrusive inconsistencies. For full transparency and to enable easy reproducibility of our methods or bespoke editing of our modifications, all changes are documented and explained in Supplementary Text S4, with the precise operational details provided in Supplementary Table SI.2. Furthermore, a visual comparison of the results is made in Supplementary Fig. S3, which demonstrates the difference in continental ε_{Nd} arrived at using purely the numerical interpolation (i.e. before making manual adjustments) compared with the refinement. Fig. 2b shows our final representation of the ε_{Nd} of the continents surrounding the ocean.

2.2.3. *Extrapolation of continental ε_{Nd} onto the continental shelf*

Once the continental interpolation was finalised, we extrapolated these data out across the marine sectors of the continental margins, adopting the philosophy that the mean ε_{Nd} signature on continental margins is similar to that of the neighbouring land surfaces. We define the extent of this extrapolation – that is, how far out to sea/how deep we can reasonably assume that the continental ε_{Nd} remains representative of the proximal marine sediments – as being limited to where sediment thickness is greater than or equal to 1000 m according to GlobSed, a total sediment thickness grid for the world's oceans and marginal seas (Straume et al., 2019). We chose to use sediment thickness to constrain our margin extrapolation as a proxy for the extent to which outcropping fields are weathered, and thus the extent to which it is reasonable to assume a similar ε_{Nd} would exist at the sediment-ocean interface. Globally, erosion, proximity to continents, transport and biogenic sedimentation determines the first order structure of sediment thickness (Straume et al., 2019). We compared extrapolating the continental ε_{Nd} out to the margins under various sediment thickness constraints ($\geq$500 m, $\geq$1000 m and $\geq$2000 m), detailed in Supplementary Fig. S5, to find the most suitable limits of our extrapolation.

Continental margins, which represent approximately 13% of the oceanic area, contain over 42% of the total ocean sediment volume, and have an estimated average sediment cover of 3044 m, in comparison with ocean crust with an estimated average sediment cover of 404 m (Straume et al., 2019). We choose $\geq$ 1000 m sediment thickness as our final extrapolation extent to encompass only marginal settings. Sediment thickness $\geq$ 2000 m did not capture all marginal settings, in particular passive margins in the Eastern Pacific and margins surrounding Australia, and we chose not to use a shallower threshold (such as $\geq$ 500 m) because this extrapolated the continental signal beyond what we deemed representative. This value was close to the average sediment cover of oceanic crust and as a result reached distal oceanic crust, for example in the western North and South Atlantic basins. We acknowledge that lithogenic input via aeolian dust flux may reach further limits than our definition, but we made the pragmatic choice to prioritise the categorisation of marginal sediments and deposits. Constraining what we define as 'continental margins' to $\geq$ 1000 m sediment thickness is, however, a somewhat arbitrary choice. Our transparent approach and fully available input data will allow future user groups to implement a different choice of delimiting sediment thickness, should they wish. The product of our final combined continental and extrapolated marginal sediment ε_{Nd} is shown by Fig. 2c.

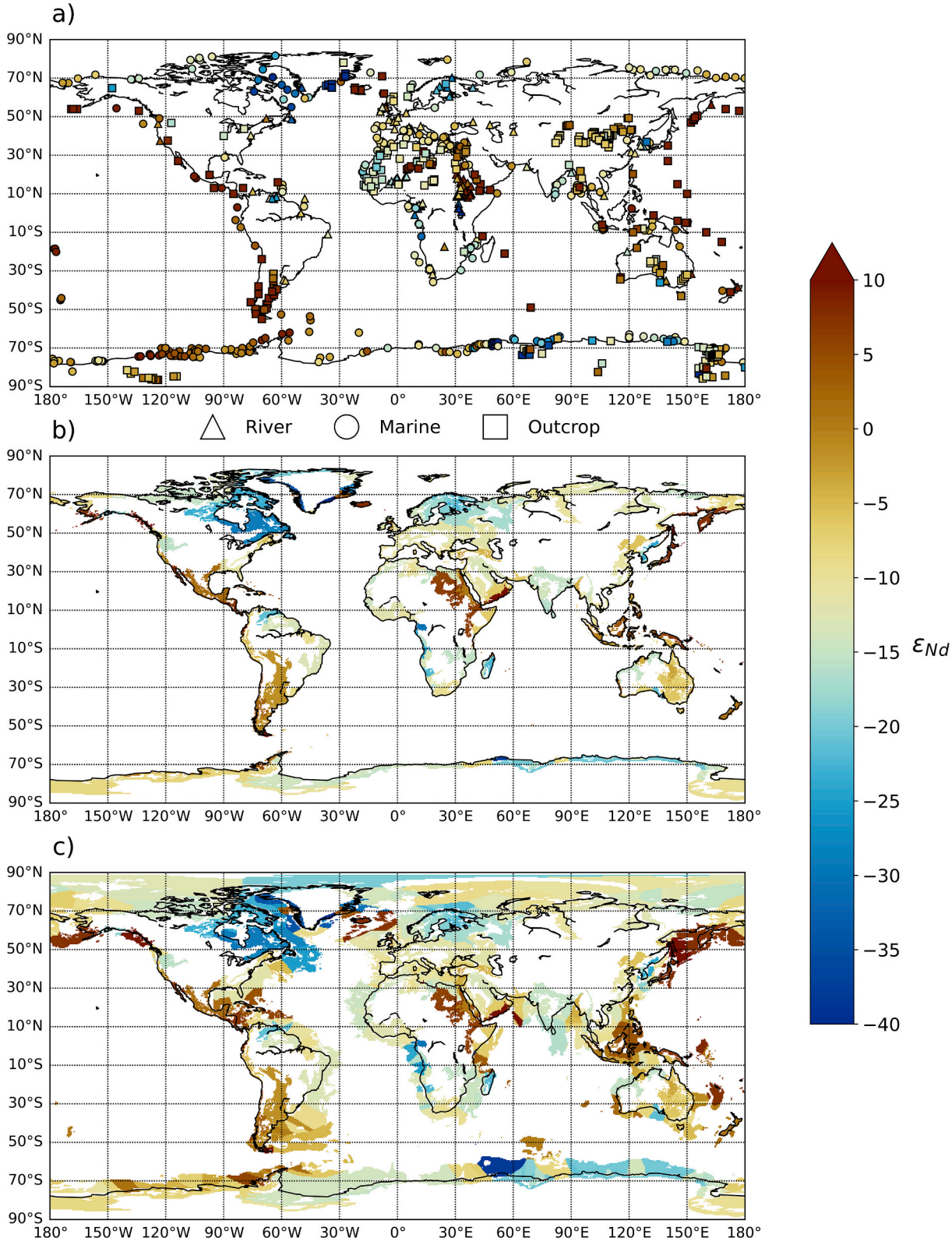

Fig. 2. Continental and proximal margin ε_{Nd} map, showing (a) sample type and ε_{Nd} of Nd isotope measurements compiled in Supplementary Table S3, indicating the three broad sample types included in the new compilation: river sediment (triangles), Holocene marine sediments (circles), and geological outcrops (squares), (b) updated continental ε_{Nd}, and (c) complete ε_{Nd} of the continents and proximal margins (constrained to where sediment thickness $\geq$1000 m).

2.3. Seafloor ε_{Nd} map

2.3.1. Data selection

In order to examine the possible role of a benthic flux on global Nd cycling and thus to test mathematically (e.g. through Nd isotope-enabled three-dimensional ocean models) the emergent hypothesis that such a flux is driven by Nd released into pore waters from detrital sediment on the seafloor during early diagenesis, the ε_{Nd} of the seafloor needs to be represented. This characterisation of ε_{Nd} across the entire sediment-water interface is also more broadly useful for investigating Nd cycling, since it allows any user to define their own (and experiment with different) depth or sediment-type boundaries for where Nd is exchanged with the water column. Based on current paradigms, it has been suggested that ideally, pore water measurements of ε_{Nd} and [Nd] would be most representative of the Nd interaction between the sediment-water interface, recording the labile Nd from detrital material into pore water (Abbott et al., 2015a; Du et al., 2020). However, to date the measurements of pore water ε_{Nd} are very spatially limited; three sites currently, all in the North Pacific, measured in near surface sediments on the continental margins between 500 and 3000 m water depth (Abbott et al., 2015b; Abbott et al., 2015a). An approach that extrapolates the few (three) valuable pore-water measurements that do exist would likely over-generalise the distribution of global labile seafloor ε_{Nd}, failing to capture a sediment-type dependent, realistic distribution even at the broad scale. Further measurements would also be needed to fully verify whether this is true.

Published detrital sediment ε_{Nd} measurements provide our most practical solution to this global open ocean pore-water data sparsity. Here, we define detrital sediments as the non-authigenic and non-biogenic sediment phases encompassing three main fractions: bulk sediment digests, decarbonated sediment residuals and decarbonated and leached sediments (hereby referred to as the detrital fraction), indicated in Supplementary Table S4 and Fig. 3a (Blaser et al., 2016; Du et al., 2016; Wilson et al., 2013). It is hypothesised that detrital sediments interact with pore water on long timescales (hundreds to thousands of years), in large part compensating for slow reaction kinetics and therefore enabling detrital sediment to exert a significant influence on the ε_{Nd} of pore water (Du et al., 2016). Furthermore, detrital sediments provide a direct measurement of the sediment ε_{Nd} in contact with pore water, albeit in the absence of quantifying exactly the reactive Nd phases. We therefore filtered the updated Nd database to identify marine core-top pore water and detrital sediment ε_{Nd} and used this compilation to produce a best estimate of the global distribution of seafloor ε_{Nd}. Similar to the continental compilation, only core-top sediments (i.e. the upper cm) or sediments deposited during the Holocene (11.7 ka to present), as well as the New Southern Ocean samples were considered, yielding a total of 1,479 observations. All the discrete marine detrital and pore water data utilised in this study are reported in Supplementary Table S4 and are shown by Fig. 3a.

Despite the development of several sequential extraction processes for the partitioning of marine sediment fractions, at present there remains no standard chemical procedure for measuring the detrital fraction ε_{Nd} of marine sediments (Bayon et al., 2002; Du et al., 2020). As such, the definitions of the three main detrital phases presented here (bulk, decarbonated and detrital fraction) represent a broad classification due to the non-uniformity in extraction methods employed within the literature. Furthermore, between these fractions, the reported ε_{Nd} may vary significantly due in part to the specific aims of the individual research efforts. For example, most (if not all) detrital samples were conducted not to establish a benthic flux of Nd to the oceans, but to understand geographical provenance and transport mechanisms (atmospheric circulation of dust, water advection, fluvial erosion, cryospheric dynamics). In all cases, the assumption is that detrital phases retain the isotopic signature of their source rock signature throughout continental weathering, sediment transport and diagenesis (e.g. Basile et al., 1997; Cook et al., 2013; Grousset et al., 1998; Grousset et al., 1992; Innocent et al., 1997; Jones et al., 1994; Grousset et al., 1988; Nakai et al., 1993; Revel et al., 1996; Simões Pereira et al., 2018; Toucanne et al., 2015; van de Flierdt et al., 2008).

Recent work suggests that strong leaching procedures in older studies could lead to loss of reactive detrital phases, which are a potentially important benthic source of Nd, and thus may not be preserved in operationally defined 'detrital residues' (Abbott et al., 2019; Abbott et al., 2016; Blaser et al., 2016; Du et al., 2016; Wilson et al., 2013). Furthermore, the standard protocols used to isolate the Fe-Mn oxyhydroxide phases in leaching procedures have been found to not only target oxyhydroxide phases, but also target clay host phases (Abbott et al., 2019). These conventional leaching methods mobilise significant quantities of silicate hosted REEs, particularly in carbonate poor sediments (Blaser et al., 2016; Wilson et al., 2013). Refined leaching methods, which now employ a gentler approach, can minimise this silicate fraction 'contamination'. Nonetheless, in the absence of a carbonate buffer, they have still been found to mobilise some of the silicate fraction (Blaser et al., 2019; Blaser et al., 2016). Utilising bulk sediment data may avoid this underrepresentation of the more labile ε_{Nd} signal and prevent removal of the clay mineral fraction ε_{Nd}. However, bulk sediment data are also relatively sparse, albeit not as scarce as pore water measurements. Acknowledging the limitations outlined above, decarbonating and leaching procedures aim to remove the preformed seawater/pore water signal in order to isolate specifically the detrital fraction, and improvements have been made towards standardising these procedures. For example, Bayon et al. (2002) presented a robust chemical procedure for separating the detrital material into decarbonated sediment residuals and specific detrital size fractions, resulting in reduced or no loss of specific phases. Within our database, decarbonated and detrital fraction observations are much more abundant, and as such, these samples are also deemed suitable for inclusion in this dataset alongside bulk sediment digests and pore-water samples, allowing for a more global representation of direct ε_{Nd} measurements covering various seafloor lithologies.

We recognise that under current practical constraints, there is no unique/ideal solution for our sample selection. To use only pore water and bulk sediment fractions would limit the number of observations to too few for producing a useful broad scale representation of the seafloor ε_{Nd} source. For example, the 106 bulk sediment observations compiled globally (compared to 541 and 829 decarbonated and detrital observations, respectively) are not only limited in number, but also are heavily biased towards marginal settings and concentrated mainly in the northwest and southwest Atlantic, the Gulf of Alaska and East Antarctica, likely underrepresenting marine sedimentary areas (e.g. deep ocean settings, the Arctic Ocean, and the Indian Ocean). On the other hand, as acknowledged by Blaser et al. (2016); Du et al. (2016) and Wilson et al. (2013), decarbonated sediment residuals and detrital fractions may (at least in some cases) provide a weaker/less significant oceanic Nd flux. Again, the available data are insufficient to fully verify this possibility or demonstrate in which specific settings it is the case. Balancing these two challenges, we made the decision to include the whole sediment (not favouring any specific detrital phases) as contributing to the sediment-water ε_{Nd}. Following further data acquisition from more labile fractions and direct comparison between the ε_{Nd} yielded by the different detrital phases of the same samples on a global scale, this approach could be revisited in the future.

2.3.2. Interpolation of seafloor ε_{Nd} map

Once an extensive compilation of suitable discrete detrital and pore water ε_{Nd} observations were obtained, the points were then interpolated globally to produce a spatially continuous ε_{Nd} signature of seafloor sediments in contact with bottom water. Again, the aim here is to broadly characterise the signature of seafloor sediments, providing a best estimate of global ε_{Nd} based on the available [and limited] dataset. Our map thus may not capture localised features and variations.

Adopting the assumption that dominant seafloor lithology types at

least partially describe the major sedimentary source and characteristics of detrital ε_{Nd}, we used a high-resolution gridded map characterising the major lithologies of seafloor sediments in the world's ocean basins (Dutkiewicz et al., 2015; see 'Seafloor Lithology Map' in Data Availability). This assumption is based on the notion that ε_{Nd} from a possible benthic flux is related to the signature and reactivity of the underlying detrital sediment, and sediments of the same lithology type likely have similar diagenetic environments. Similar to the digital geological map used for continental margin ε_{Nd} (Section 2.2.2), this provided a spatially delimited mask of polygons capturing the broad distribution of seafloor sediment types. We used this mask to inform the interpolation of discrete data onto a continuous high-resolution grid by constraining the nearest-neighbour extrapolation of individual measurements to keep within the limits of each polygon. Thus, we implicitly assume that proximal sediments of the same depositional type contain similar Nd characteristics, with hard boundaries where the sediment type changes, although there is no imposed relationship between distal polygons of the same sediment type in this objective numerical method.

Diagenetic reactions in sedimentary deposits are reliant on the properties of the depositional environment. Biogenic debris in particular are often inherently unstable, with organic matter, carbonate and opaline silica as dominant biogenic solids involved in early diagenetic reactions (Jahnke et al., 1989). Thus, the contribution of particular biogenic phases to early diagenetic processes is highly complex and requires a thorough understanding of the behaviour of each biogenic component and the depositional environment in which digenesis occurs.

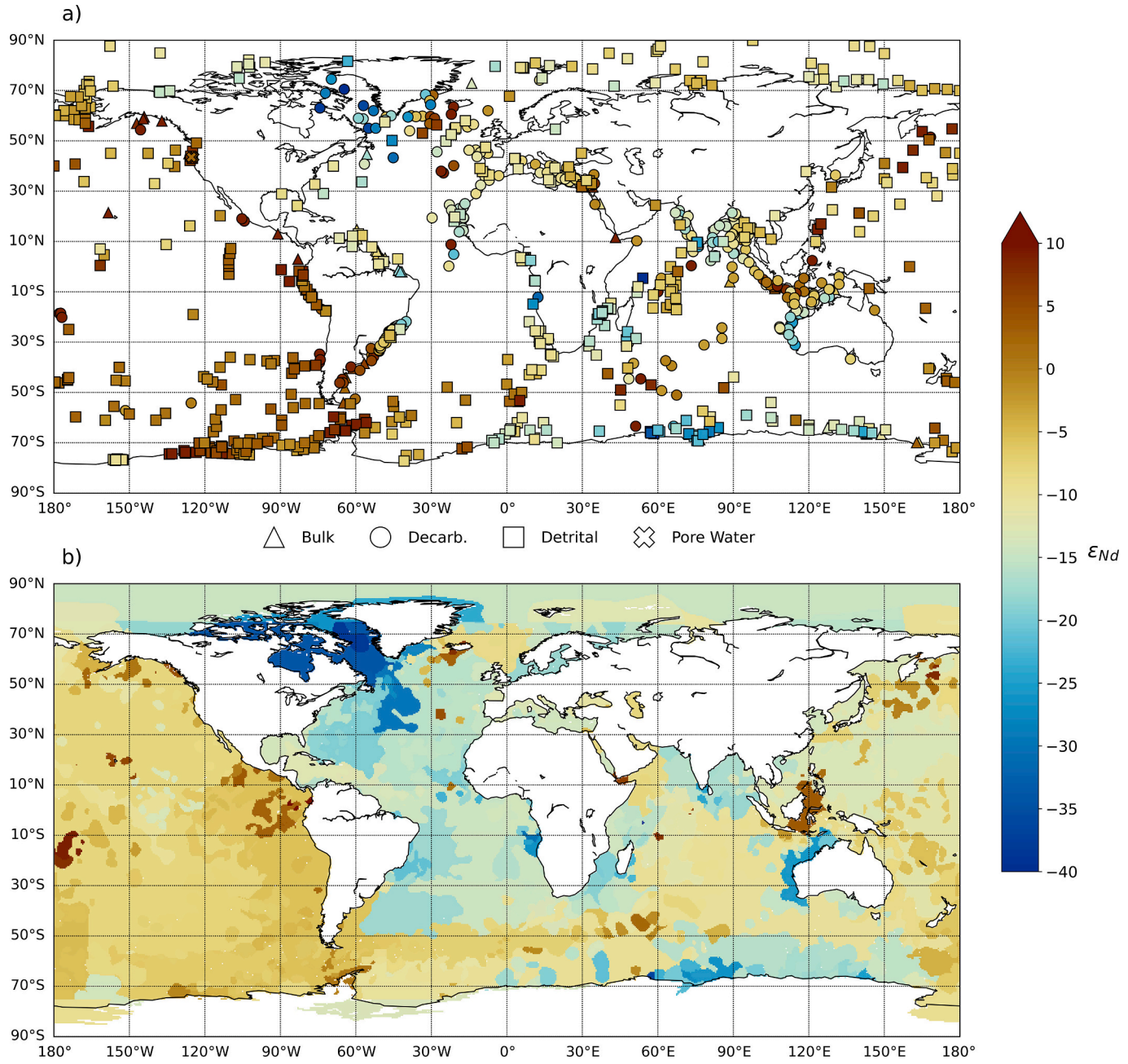

Fig. 3. Seafloor sediment ε_{Nd} map. (a) Location and ε_{Nd} of the discrete marine detrital and pore water data compiled in Supplementary Table S4 and used to produce a best estimate of spatially continuous seafloor ε_{Nd}. The three broad sample types of marine detrital and pore water data included in the compilation are indicated: bulk sediment digests (triangles), decarbonated sediment residuals (circles), specific detrital size fractions (squares), and pore-water measurements (crosses). (b) Spatially continuous seafloor ε_{Nd} representation interpolated from the discrete data.

Recent pore water and water-column [Nd] observations from the Tasman Sea have highlighted the possibility that regions dominated by biogenic carbonates can be important contributors to the global benthic flux (Abbott, 2019). Due to low [Nd] in biogenic sediments, these sediment regions had previously been dismissed as a likely contributor to the oceanic Nd budget (Abbott et al., 2015b). However, a diffusive flux of Nd calculated in this region, although smaller, was similar in magnitude to that measured in the low-carbonate samples measured from the North Pacific. Such data may provide evidence for expanding the area over which we consider the benthic flux to be an important contributor to marine ε_{Nd}, and further suggests that a benthic flux may be driven by a small fraction of the sediment (i.e. dissolution of clay fraction) (Abbott, 2019; Abbott et al., 2019; Huck et al., 2016).

In order to enable the testing of a global benthic flux, an ε_{Nd} signature therefore needs to be assigned to all depositional sedimentary environments. Here, we chose not to make assumptions regarding early diagenetic reactions and how they might alter Nd fluxes within different depositional environments, and instead applied the same method to characterise all sediment ε_{Nd}. This approach was adopted in order to limit the complexity of a method that is necessarily based on sparse data, including reducing the number of arbitrary assumptions we would otherwise be required to make. This has the benefit of producing a more reproducible data product and methodology, which can then be adapted by any user in the community according to our evolving understanding of the role of particular biogenic phases in early diagenetic processes, the role of a benthic flux within diverse sediment compositions and depositional environments, and the wider acquisition of suitable measurements. Note, that for pore water measurements, we use the mean of all depths in the upper 11.1 cm of seafloor sediment for each site, representing all available data (see Supplementary Table S4). This seems justified as the average ε_{Nd} of pore water is found to be near constant with depth at each site (Abbott et al., 2015a).

In certain poorly documented areas and where the interpolation failed to capture a representative ε_{Nd} based on what is known to exist, manual adjustments were made. These modifications follow a similar approach to that described in Section 2.2.2 and are based on available observational and expert evidence, including (i) consideration of the source and location of detrital input to the region, (ii) the assumption that the mathematical means of the available data best represent domains containing a large number of data points, and (iii) spatially constraining localised extreme ε_{Nd} signals, e.g. from volcanic island arcs, which are not always captured in the mask of major sediment lithologies. All changes are explained in Supplementary Text S4 (with precise operational detail for how to implement/revert them in Table SI.3), alongside graphical depictions of the new gridded seafloor ε_{Nd} dataset that show the direct output of the numerical interpolation schemes before expert manual adjustments were made compared with the refined version (Supplementary Fig. S4). Fig. 3b shows our final, refined representation of the ε_{Nd} of seafloor sediment.

3. Results

3.1. Continental ε_{Nd} representation

Similar to Jeandel et al. (2007), we focused our spatially continuous reconstruction of continental ε_{Nd} on the regions surrounding the ocean (as shown in Fig. 2b), since the main purpose is to provide updated information for examining *marine* Nd cycling. Thus, the continental interiors are largely omitted from our final ε_{Nd} distribution.

Examination of the variability in our updated map of continental ε_{Nd} reveals the expected pattern of the most negative values corresponding to known provinces of the oldest unradiogenic continental rock worldwide (e.g. the exposed Archean rock comprising the North Atlantic Craton around southwestern Greenland and Paleoproterozoic granites which constitute the Rae Craton that forms Baffin Island and parts of western Greenland), and positive values corresponding to young volcanic arcs (e.g. convergent margin volcanism in the northwest Pacific) and hotspot/ocean island volcanics (e.g. the Hawaiian Islands Archipelago, the Samoan Islands and the Kerguelen Islands).

For instance, in the high northern latitudes, continental crust surrounding the Hudson Bay and Labrador Sea in eastern Canada and western Greenland display largely unradiogenic values of -25 ε_{Nd} due to the presence of old Archean and Proterozoic units. This characterisation of very negative (-25) ε_{Nd} has been observed recently in a regional North Atlantic marginal ε_{Nd} map produced utilising compiled Holocene bulk surface sediments by Stichel et al. (2020). Similarly, here, the most unradiogenic signals correspond particularly to crust exposed on the North Atlantic Craton, where these lithological units are amid some of the oldest rocks worldwide. Previous investigations from Innocent et al. (1997) on modern and late Quaternary sediments in the northwest North Atlantic further highlight the most unradiogenic ε_{Nd} signals (ranging from -35 to -24) within sediments from terrains belonging to the North American Shield, particularly Baffin Island, Quebec and Labrador regions. Accordingly, these regions are characterised in our continental representation by ε_{Nd} ranging -32 to -23. Conversely, recent volcanic intrusions associated with the younger Cenozoic mafic rocks in Iceland and from the Nansen Fjord in East Greenland yield radiogenic ε_{Nd} signatures ranging from +4 to +7. In particular, exposed Holocene basalts on the continental shelf associated with Icelandic volcanism results in a radiogenic signal of +7 over Iceland, a value consistent with the first-order estimation of the Icelandic detrital Nd source signal to the ocean from Innocent et al. (1997) of +8. Material eroded from Iceland has particularly high [Nd], and so even a small contribution from this mafic sediment to seawater can have an important role governing Nd distributions here and thus an important region to characterise (Stichel et al., 2020).

The Arctic Archipelago displays an east-west gradient in ε_{Nd}, with unradiogenic values of -23 ε_{Nd} in the southeast associated with the oldest rocks of Archean and Proterozoic origin and less unradiogenic values of -12 ε_{Nd} towards the northwest of the archipelago related to Palaeozoic crust. Continental crust of lower Palaeozoic origin in northern Alaska has unradiogenic values of -14 and in northeast Siberia, proximal to the East Siberian Sea, younger Mesozoic units have more radiogenic values of -7. Asahara et al. (2012) analysed detrital fraction ε_{Nd} from marginal sea sediments in the Arctic to identify sources of terrigenous detritus in the Bering and Chukchi Seas. The authors found ε_{Nd} in detrital fractions in the Chukchi Sea range from -10 to -8, which they attributed to terrigenous detritus material derived from northeastern Siberia (-9), and additionally from the Mackenzie River basin including the Canadian Shield (-14). Detrital fractions in the eastern Bering Sea are varied, though generally more radiogenic (-9 to +3), representing terrigenous input from the Yukon basin, underlain by Mesozoic and Palaeozoic rocks from Alaska (-9) and the Aleutian-arc volcanics (+7). Our continental representation in this region corresponds well to these previous estimations, suggesting that the spatial heterogeneity within continental ε_{Nd} in this region is captured reasonably well, which is especially important for the Arctic Ocean, whose water column Nd distributions are distinctly and generally influenced by the broad, surrounding continental shelves (Porcelli et al., 2009).

There is less spatial ε_{Nd} variability in the rest of the Siberian margin, central and southern Europe, and North, West and South Africa, which all display a relatively spatially homogenous ε_{Nd} signal between -11 and -7, with the more radiogenic values associated with widespread Cenozoic and Mesozoic rocks in these regions. A previous study by Revel et al. (1996) measured the ε_{Nd} of lithogenic particles from a sediment core in the Icelandic basin to trace its detrital origin. The authors reported ε_{Nd} of -12 originating from the British Isles, a value consistent with our characterisation (-12 to -11). Measurements from Scandinavia, on the other hand, are quite unradiogenic, with the most negative values of -23 ε_{Nd} found in Archean rock in Finland and values of -22 to -14 in Proterozoic rocks within Norway and Sweden. These unradiogenic values correspond to findings by Bayon et al. (2015) who assessed the ε_{Nd} of

sediments collected in Finland near the Kiiminkijoki river mouth, which drains the Precambrian shields of Fennoscandia, reporting ε_{Nd} of -23. Further, Revel et al. (1996) reported ε_{Nd} in lithogenic particles on the Norwegian margin around -19, consistent with our continental characterisation here.

Looking at the African continent, Scheuvens et al. (2013) reported bulk ε_{Nd} of dust in northern Africa to evaluate lithogenic sediments, measuring ε_{Nd} of -15 to -10 in Southern Algeria and northern Mali. Furthermore, samples collected off the west coast of northern Africa ranged between -16 and -8, these values are in agreement with our continental representation of this region (-14 to -13) illustrating the ε_{Nd} characteristics here have been effectively captured. On the other hand, north-eastern Africa displays quite a comprehensive picture of positive ε_{Nd}, in particular around the Ethiopian Highlands and the Red Sea region, related to magmatic rifting (0 to +6). Overall, across the mainland of northern African a eastward tendency of increasing ε_{Nd} occurs. This gradient has been observed previously in detailed studies of terrestrial and marine sediments (Blanchet, 2019; Scheuvens et al., 2013).

The east coast of USA, Brazil and Uruguay are similar in regard to the intermediate values across the majority of Europe and West Africa, with ε_{Nd} generally falling within the -14 to -10 range, here Caledonian and Hercynian rocks cover the majority of these continental areas and so share broadly similar ε_{Nd} characteristics (Jeandel et al., 2007). However, characterisation of the east American continent is based on few observations and may underrepresent the true spatial variability of those regions. Examining river sediment ε_{Nd} from the Amazon and Mississippi river mouths, Bayon et al. (2015) reported values of -11 and -12 to -11 respectively, which correlate well with the continental ε_{Nd} interpolation at the location of these two river mouths. This is an important feature to capture, because these large river systems deliver large inputs of terrestrial particulate material to the ocean.

The geology of the west coast of the Americas and throughout central America is complex, associated with divergent and transform boundaries. Nonetheless, ε_{Nd} measurements on the Pacific Rim are consistently radiogenic, ranging from around +2 to +10 in the Cenozoic units there. Grasse et al. (2012) reported radiogenic measurements of ε_{Nd} (-2 to +3) and increased [Nd] in surface waters in the Eastern Equatorial Pacific, indicating exchange with either volcanic particles in the water column or highly radiogenic shelf sediments. These surface waters are characterised by increasingly radiogenic ε_{Nd} as we head northwards up the coast from Peru to Ecuador. A radiogenic gradient in continental ε_{Nd} is also represented here, ranging from -5 in Peru to +7 in Ecuador. Out in the Pacific, the Hawaiian island chain and other active volcanic island chains yield ε_{Nd} values at the top end of our scale (+8 to +10). Here, values for the volcanic islands on the Hawaiian plume (+7 to +9) are in agreement with present day (0 ka) ε_{Nd} measurements compiled and summarised by Bryce et al. (2005), with mean ε_{Nd} values measured on Mauna Loa (+5), Hualalai (+6), Kilauea (+7) and Mauna Kea (+8). The detail of these small volcanic island chains (including Hawaii, Tahiti, Gallapagos, etc.) is not fully evident in the global image shown in Fig. 2b, but can be accessed by downloading the high-resolution vector datasets accompanying this study (Supplementary Dataset S1).

India and Sri Lanka are characterised by a relatively homogenous unradiogenic ε_{Nd} signal of -16 associated with Proterozoic and Pan-African rocks. Chemical weathering of the Himalayan system exports large sediment loads to coastal regions via the Ganges-Brahmaputra Rivers, Lupker et al. (2013) compiled measurements of ε_{Nd} in river sediments in the Ganges and Brahmaputra Rivers highlighting unradiogenic values of -18, and a range of -14 to -19 respectively. Our continental characterisation in margins surrounding the Bay of Bengal (-15) falls within the range of ε_{Nd} characteristics from these major river systems. Moreover, Thailand, with predominantly upper Palaeozoic units, is characterised by values of -14, and younger crust (predominantly of Mesozoic origin) comprising Cambodia and Vietnam have values of -9. A previous study by Peucker-Ehrenbrink et al. (2010) explored the relationship between bedrock lithology and age to estimate the ε_{Nd} of large-scale continental drainage regions. Here, the ε_{Nd} of Southeast Asia was estimated to be -14. Palaeozoic crust in North and South Korea yield more unradiogenic ε_{Nd} values of -20 to -16, whereas Japan, Indonesia and the Philippines bear a very radiogenic signal around +5, associated with active plate tectonics and recent Cenozoic formations. The basaltic composition of numerous islands located in the southwestern intertropical Pacific (e.g. Papua New Guinea, Solomon Islands, Fiji) yield radiogenic ε_{Nd} (ranging +5 to +7). Grenier et al. (2013) compiled ε_{Nd} data from rock and sediment samples to characterise the average ε_{Nd} of such islands. Radiogenic mean ε_{Nd} of +8, +7 and +8 were attributed to Fiji, Vanuatu and Tonga respectively, in accordance with our representation of ε_{Nd} here. The authors further suggest that these islands provide an important lithogenic supply of radiogenic ε_{Nd} to the south-western Pacific. In comparison, the geology of Australia is broadly characterised by several Archean and Middle Proterozoic cratons, with younger formations of Phanerozoic age occurring mainly in north Australia (Ehlert et al., 2011). In our continental ε_{Nd} representation, north-eastern and eastern Australia and Tasmania display a relatively homogenous signal with Cenozoic and Mesozoic rocks dominating, and thus yielding values of around -8 to -6. The presence of Proterozoic to Archean units in north-western Australia and southern Australia provide two relatively spatially constrained regions of quite unradiogenic ε_{Nd} (-20 to -15).

Antarctica displays a high degree of spatial heterogeneity, this heterogeneity has been observed previously in studies documenting the variability of Antarctic sediment sources using $^{40}Ar/^{39}Ar$ ages and bulk < 63 μm Sm/Nd isotopes (Roy et al., 2007; Simões Pereira et al., 2018). This observed systematic variability is in agreement with known major geological events that characterise Antarctica's bedrock. Broadly the geology of Antarctica is naturally divided into East and West Antarctic domains, East Antarctica is a complex Precambrian craton comprising Archean terrains separated by Proterozoic units, while West Antarctica is characterised through abundant late Mesozoic-Cenozoic intrusive volcanic rocks around Palaeozoic and Mesozoic crust (Roy et al., 2007). In our continental ε_{Nd} representation here, the most unradiogenic values occur across East Antarctica, with a general signal around -20 within predominantly Proterozoic and Archean crust, the most unradiogenic signal of -38 is found within the Archean units of Enderby Land. Radiogenic values around -5 are found in West Antarctica, representing younger crustal ages of Mesozoic and Cenozoic rock, with the most radiogenic signal in this region (+5) occurring within Cenozoic and extrusive volcanic rocks on the Antarctic Peninsula. Intermediate values occur in our characterisation of continental and marginal rocks surrounding the Weddell Sea (-14) and the Ross Sea (-8). In these regions, there is a degree of variability among Holocene marine sediments (ranging -10 to +2 (detrital fraction) and -28 to -11 (in decarbonated and detrital fractions) within the Weddell Sea and Ross Sea respectively), which is important, because they are the main sample types used to characterise these regions. In the Weddell Sea, this variability likely represents detrital contributions from proximal rocks off the Antarctic Peninsula (in the absence of continental samples, the nearest marine sediments (detrital fraction) to these rocks range from -6 to +1), and bordering crust from East Antarctica (nearby marine sediments (detrital fraction) to the continents range -15 to -10). In the Ross Sea, the variability likely reflects detrital inputs from the bordering continental crust of East Antarctica (-15 to -6 in bulk rock samples) and West Antarctica (-9 within bulk rock samples).

3.2. Seafloor ε_{Nd} representation

Consistent with the distribution of continental ε_{Nd}, the most unradiogenic sediment in our seafloor compilation (summarised in Fig. 3b) is found in the northernmost North Atlantic sector, specifically in Baffin Bay, the Hudson Bay and the Labrador Sea, where ε_{Nd} values range from approximately -28 to -25, reflecting deep-sea detrital input from surrounding unradiogenic continental crust. Similarly, but at the opposite

end of the scale, more radiogenic ε_{Nd} of +3 to +7 is observed in the ocean sediment surrounding Iceland as a result of detrital input from recent volcanism. Further south and away from the coast, our interpolation produces a generally more moderate signal of -13 to -11 ε_{Nd} in the Atlantic Ocean sediments. The Gulf of Mexico/Caribbean Sea contain some of the more radiogenic sediments (-10 to -9), but otherwise in the open Atlantic, there is a slight gradient from more unradiogenic values in the northwest to more radiogenic values approaching the Southern Ocean and Namibia/South Africa in the southeast. However, we note that the deep Atlantic Ocean is the most data sparse region in our database, especially in the open South Atlantic. Further data acquisition in this area could alter our results.

The Mediterranean region is data rich, due to the detailed wealth of published observations gathered by Blanchet (2019) in addition to detrital measurements accompanying the data presented by Tachikawa et al. (2017). The Mediterranean Sea is mainly characterised by an unradiogenic sediment signal of -11, consistent with the majority of observations here, with an exception being in the east of the basin, located north of Egypt, at the mouth of the Nile River. Here, multiple observations range from -5 to -2 and the area is broadly characterised by an ε_{Nd} signal of -3. These higher values trace the delivery of radiogenic sediments by the Nile Rivers to the Eastern Mediterranean from Cenozoic volcanic plateaus of the Ethiopian Highlands (Fielding et al., 2017). The Mediterranean Sea communicates with the eastern North Atlantic via the Strait of Gibraltar, with Mediterranean Outflow Water believed to be an important modulator of the North Atlantic salt budget (Tachikawa et al., 2004; Voelker et al., 2006). This water mass forms seasonally in the east of the basin, where an ε_{Nd} gradient towards more radiogenic values occurs, and is thus an important feature for understanding the sediment-water interaction on the ε_{Nd} of Mediterranean Outflow and Atlantic Surface Water in the Mediterranean (Ayache et al., 2016; Tachikawa et al., 2004).

In the Indian Ocean, as already described in Section 3.1, unradiogenic detrital sediment is sourced by chemical weathering in the Himalayan system transported to the oceans via the Ganges-Brahmaputra Rivers (Lupker et al., 2013), and provides a localised source of -14 in the Bay of Bengal, a similar signal also persists close to the western coast of India. Notwithstanding, most of the Indian Ocean away from the continents is characterised by a more intermediate signal ranging from -9 to -7. In proximity to the western coast of Australia, the ε_{Nd} of clay size sediment fractions range from -22 to -8, a result of erosional supply off adjacent landmasses and surface hydrography, with the most unradiogenic (decarbonated) detrital sample (-22) off Cape Basin reflecting riverine input of weathered Archean rock from the Pilbara Craton (Ehlert et al., 2011). Overall, the seafloor sediment in this region is characterised by an ε_{Nd} of -21 due to the transport of weathered fine-grain material from coastal Proterozoic and Archean regions of northwest and west Australia, by the southward flowing Leeuwin Current, which is the dominant poleward near-coastal current in this region (Ehlert et al., 2011).

Much more radiogenic signals (+4) are observed surrounding Indonesia and the Philippines, reflecting detrital input derived from surrounding radiogenic Cenozoic units forming the Indonesian Archipelago, particularly arc, hotspot volcanics and oceanic plateaux in eastern Indonesia (in particular, the Ontong Java Plateau), and further detrital input from the Philippine Islands, one of the main sources of deep-sea sediment in the west Philippine Sea (Hall, 2002; Zhang et al., 2020). Radiogenic signals (+6) are observed locally in the Arabian Sea of the Indian Ocean surrounding the Maldives, caused by detrital input from the Maldives and surrounding basalts underlying the atolls, which formed in the Mesozoic Era (Gischler, 2006). In the western and north-central Pacific, aeolian dust from Asia, the second largest dust source area on Earth, contributes significant terrigenous material to the seafloor (Han et al., 2011; Nakai et al., 1993), providing an ε_{Nd} signal of approximately -10. On the other hand, eastern Equatorial and South Pacific sediments are more radiogenic, ranging from -6 to -4 in the deep ocean, with more radiogenic signals observed closer to the continents and on the circum-Pacific ring of fire.

For the high latitudes, in the Arctic Ocean, away from the continental margins, the seafloor has an ε_{Nd} of -12, consistent with the majority of detrital observations here. In the basin of the Chukchi Sea, ε_{Nd} is -7, influenced here by terrigenous detrital input from north-eastern Siberia, input from the Yukon River via Bering Strait inflow and from the Mackenzie River Basin containing input from the Canadian Shelf (Asahara et al., 2012; Haley and Polyak, 2013). Surrounding the western edge of the broad Eurasian shelf and Svalbard seafloor sediment ε_{Nd} is -10, whereas north of Greenland ε_{Nd} is characterised by a more unradiogenic signal of -20, resultant from detrital input from surrounding continental sources (Maccali et al., 2013). The Nordic Seas have a predominant ε_{Nd} signal ranging from -13 to -11, with a less negative signal (-6) observed in ocean sediment within the Irminger Basin, associated with detrital input from mafic source rock from Iceland and Western Greenland (Stichel et al., 2020). Based on the available data, we characterise much of the Southern Ocean seafloor ε_{Nd} to have a relatively intermediate signature (typically -8 to -5), but with more unradiogenic values of -12 proximal to East Antarctic shorelines and more radiogenic values of around -4 surrounding West Antarctica.

4. Discussion

4.1. Combined representation of the ε_{Nd} signal at the sediment-water interface

In this study, we have presented an updated compilation of current measurements of a range of possible sources of Nd isotopes to the ocean, and we have used this new synthesis to produce a spatially continuous dataset of seafloor and continental margin ε_{Nd}. In so doing, we provide suitable data products to facilitate a step-change in our ability to address outstanding questions concerning marine Nd cycling (e.g. through new conceptual or three-dimensional ocean modelling) and a methodology for reproducing/adapting our results.

The possible existence of a benthic flux of Nd to overlying waters, or simply a less spatially constrained boundary exchange at the sediment-water interface than has previously been adopted in most modelling studies (Arsouze et al., 2009; Arsouze et al., 2007; Gu et al., 2019; Rempfer et al., 2011) brings forth the requirement for global mapping of seafloor ε_{Nd}. We undertook this exercise, utilising all of the available data that we are aware of at the time of writing to produce our final, spatially continuous distribution (Fig. 3b). However, we acknowledge that we may have missed some sites, and we hope that when spotted, others will contribute these to the continually evolving database first published by Blanchet (2019) (see Data Availability). There are most certainly underrepresented regions in our compilation of measurements – notably, huge swathes of the open Atlantic Ocean, deep Pacific, and southern Indian Ocean – which we hope may become better represented in time (notwithstanding the practical difficulties associated with very deep ocean sampling), thus enabling a more thorough capturing of the spatial distribution of seafloor ε_{Nd}. Furthermore, as research continues, it may become more practical to further filter the available data to use only the most suitable sediment sources (ultimately, pore waters or specifying precisely the labile Nd fractions; see discussion in Section 2.3.1, above). Nonetheless, it is a testament to the hard work of the wide research community that so many observations do already exist, enabling us to produce our best estimate of seafloor ε_{Nd} from these data.

The final step is to bring the two data products together, and Fig. 4 shows our combination of the continental margin and seafloor ε_{Nd} distributions. This dataset can be considered to be our best estimate of the global distribution of ε_{Nd} at the entire sediment-water interface to date. To produce this final characterisation of global seafloor sediment ε_{Nd} distributions, we used the continental ε_{Nd} map extrapolated to where sediment thickness $\geq$ 1000 m, and the remaining sediment regions are represented using the seafloor ε_{Nd} map. The signal varies spatially, but in

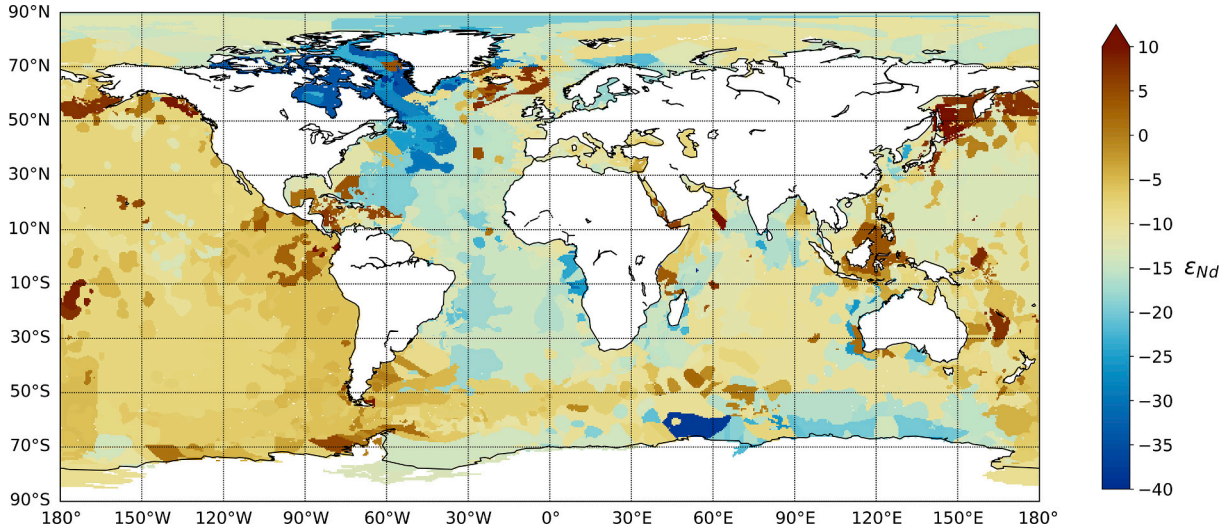

Fig. 4. Nd-isotope signature of the global sediment-water interface, showing the combination of the seafloor ε_{Nd} and the continental margin ε_{Nd} maps. This final characterisation of global ε_{Nd} distributions at the sediment-ocean interface uses the continental ε_{Nd} map extrapolated to where sediment thickness $\geq$ 1000 m, and the remaining sediment regions are represented using the seafloor ε_{Nd} map.

very general terms, the North Atlantic provides an unradiogenic signal, intermediate values occur in the Indian and Southern Oceans, and the most radiogenic values occur in the Eastern Equatorial Pacific, Southern Pacific and circum-Pacific ring of fire.

4.2. Comparison with previous compilation of continental margin ε_{Nd}

Fig. 5 shows the difference in ε_{Nd} between the previous, seminal map of continental ε_{Nd} produced by Jeandel et al. (2007) and the new distribution presented here. With positive [negative] values showing regions where our newer ε_{Nd} representation has a more radiogenic [unradiogenic] signal compared with the previous map. In this section, we discuss key updates to the original continental ε_{Nd} map, addressing improvements and further illustrating regions where data limitation causes outstanding uncertainty. Overall, our updated compilation has vastly increased the number of suitable continental ε_{Nd} observations and also improved the spatial coverage of ε_{Nd} observations, with an extra 855 samples in addition of those used in Jeandel et al. (2007). This has enabled a more data constrained representation of continental ε_{Nd} (see Supplementary Fig. S6).

Broadly in comparison to Jeandel et al. (2007), the new continental ε_{Nd} map is more radiogenic in the Arctic Shield, Northern Eurasia, South America, north-eastern Africa and Antarctica, and has more unradiogenic values over southern Greenland, north-eastern Europe, western and eastern Africa and parts of the Americas. Jeandel et al. (2007) noted that in the previous ε_{Nd} representation, certain regions were data limited and so broad estimations had to be made, for example continental rock in Alaska, northern Eurasia, Pakistan, Cameroon, Somalia and Brazil. In Fig. 6, we show the new continental ε_{Nd} representation in regions where we consider a higher number of observations have improved the characterisation of ε_{Nd} relative to Jeandel et al. (2007), as explained in more detail below, with a particular focus on regions considered important for deep-water formation and thus potential ε_{Nd} labelling of water masses by continental erosion.

Newly compiled observations around the Arctic within this study (Fig. 6a) have led to a more detailed representation of the continental

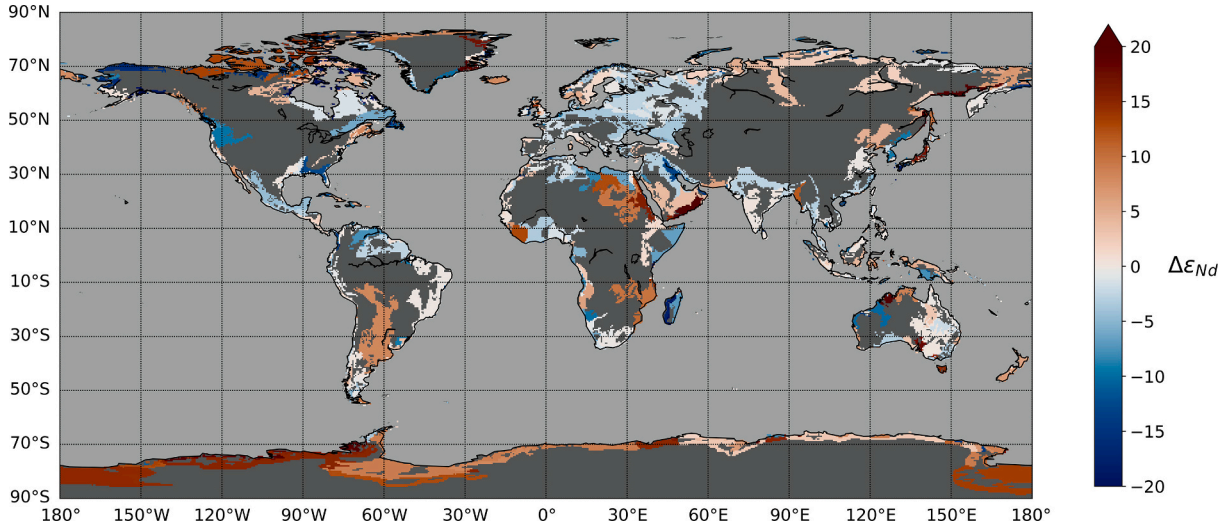

Fig. 5. Difference in ε-units between the continuous representation of continental ε_{Nd} presented in this study and the previous map produced by Jeandel et al. (2007). Positive [negative] values show regions where our newer ε_{Nd} interpolation has a more radiogenic [unradiogenic] signal compared with the previous map; no data regions are coloured dark grey (land) and light grey (ocean).

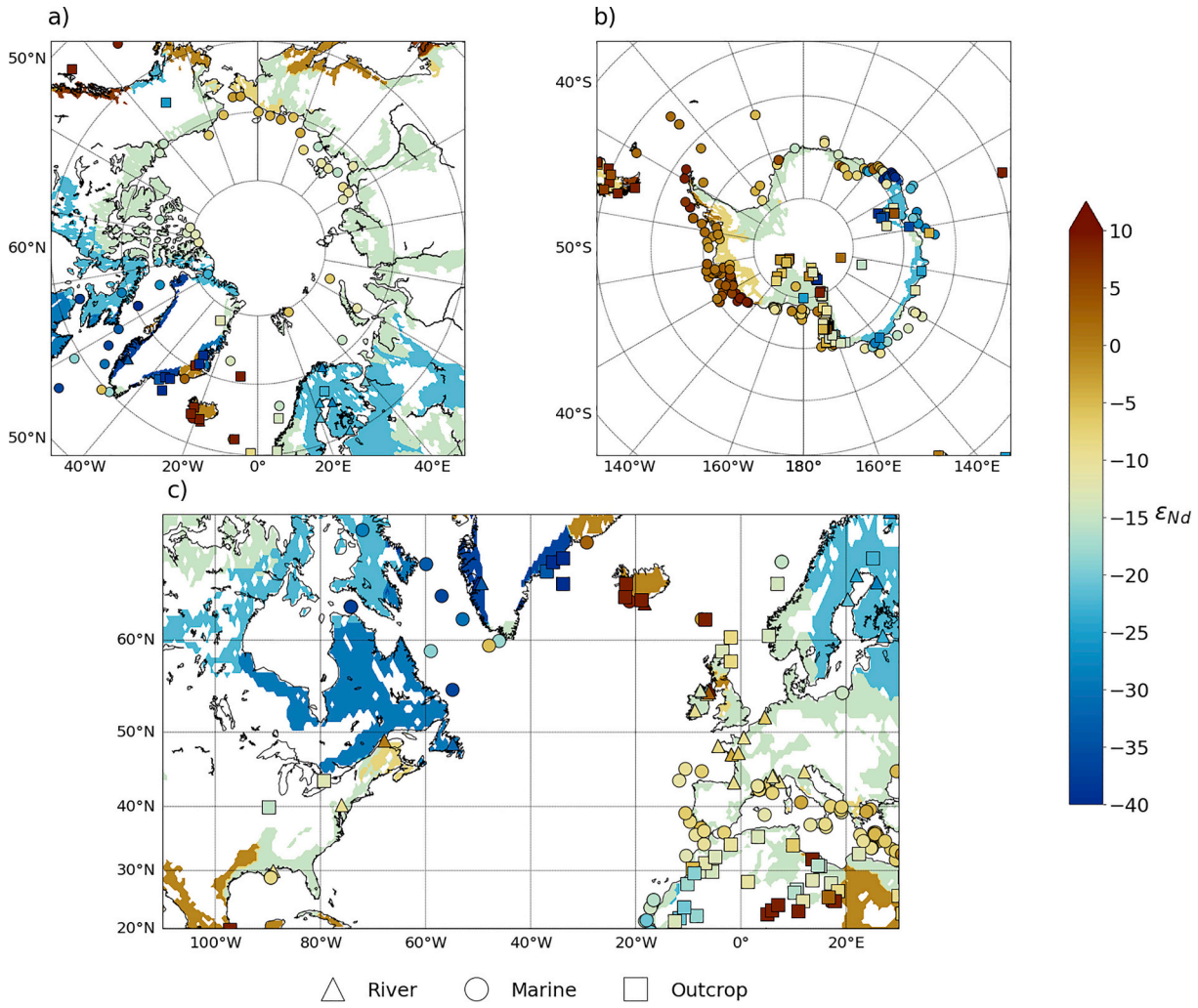

Fig. 6. Regional analysis of the new continental ε_{Nd} map, with particular focus on regions important for deep-water formation and thus potential ε_{Nd} labelling of water masses by continental erosion. The displayed regions have reduced uncertainty in the characterisation of ε_{Nd} relative to the original maps produced by Jeandel et al. (2007; not shown) in large part due to an increased number of observations. (a) The polar Arctic region, (b) Antarctica, and (c) the North Atlantic, overlain by the discrete ε_{Nd} measurements used in the interpolation presented here and also indicating the three broad sample types included in the new compilation: river sediment (triangles), Holocene marine sediments (circles), and geological outcrops (squares). For further context, an equivalent version for the new complete ε_{Nd} representation of the sediment-ocean interface (i.e. including the whole ocean floor), both from the seafloor-only data and from combining the seafloor and continental interpolations based on sediment thickness (see Section 4.1), is provided in Supplementary Fig. S7.

ε_{Nd} in the new map. This was a particular region of uncertainty in Jeandel et al. (2007), especially across northern Alaska and north-eastern Eurasia where there were previously no observations. These areas now have a multitude of continental measurements and the region is characterised by a more radiogenic signal than was previously estimated, with the signal from northern Alaska updated from -29 to -15 and north-eastern Eurasia from -14 to -12. The additional seafloor ε_{Nd} map adds further previously uncharacterised detail to the region, utilising additional marine detrital samples from seafloor sediment in the Arctic (shown Supplementary Fig. S7a). Here, the Arctic seafloor sediment-water interface is broadly characterised by an ε_{Nd} of -12, with more unradiogenic marginal values (-20) north of the Canadian Shield and northern Greenland.

A large contrast and increased spatial detail occur in the Antarctic region (Fig. 5), driven by the greater number of observations now available (Supplementary Fig. S6). Fig. 6b highlights the improved data density and coverage of observations, particularly in East Antarctica (notably around Prydz Bay and Enderby Land), Victoria Land, the Ross Ice Shelf and the Antarctic Peninsula (especially to the west of the peninsula, surrounding the Bellingshausen Sea). Enhanced availability of data has enabled a better constrained characterisation of the ε_{Nd} of Antarctica. However, there still remains data scarcity around Ronne Ice Shelf in the Weddell Sea, and so our representation of ε_{Nd} is more uncertain here. In comparison to the Antarctic ε_{Nd} presented by Jeandel et al. (2007), the Antarctic Peninsula, the Ross Sea and the Weddell Sea are much more radiogenic in our interpolation of measured ε_{Nd}; +5, -8 and -14 respectively as opposed to the previous more homogenous estimate of -23. East Antarctica remains unradiogenic with values around -20, and the most unradiogenic signal (-38) occurs in the Archean Napier Complex of Enderby Land, East Antarctica.

Antarctic Bottom Water ε_{Nd} measured close to the Antarctic shelf is believed to be influenced by marginal sediment inputs, evidenced by increased [Nd] closer to the continent. Lambelet et al. (2018) found seawater measurements in proximity to the Antarctic coast also display spatial heterogeneity, carrying Nd isotope fingerprints that are characteristic of their formation area and consistent with the heterogenous ε_{Nd} signal presented in our continental representation. In this study, Adélie Land Bottom Water samples were found to reflect unradiogenic ε_{Nd} of surface sediments collected around East Antarctica, particularly detrital measurements from the Adélie Craton (-20). Ross Sea Bottom Water

reflected the radiogenic fingerprint of West Antarctic lithologies, with detrital measurements ranging from -6 to +2 and newly formed Weddell Sea Bottom water was influenced by unradiogenic inputs from old continental crust in the East Antarctic part of the Weddell Embayment.

This better constrained representation of Antarctic and Southern Ocean ε_{Nd} may be an important update for understanding ε_{Nd} cycling in the ocean, especially if these data are used as boundary conditions for Nd-isotope models. The updates from our compilation and interpolation are particularly useful because the formation of modern Antarctic Bottom Water (AABW), which is a key component of the global oceanic overturning circulation, forms predominantly in the Ross and Weddell Seas and around the much more unradiogenic East Antarctic margin from the Adélie Coast to Prydz Bay. Thus, here, the ε_{Nd} signal from the continents and seafloor sediment may exert a strong influence on seawater ε_{Nd} provinciality, as pointed out by Lambelet et al. (2018). Furthermore, the strength and location of the boundaries of the Antarctic Circumpolar Current (ACC) are important parameters for understanding the role of the Southern Ocean in global climate change (Hemming et al., 2007). For example, it has been suggested that glacial stratification and/or variations in sea-ice cover in the circum-Antarctic may play an important role in glacial variations in atmospheric pCO_2 (Sigman et al., 2004; Stephens and Keeling, 2000). In this context, northward displacement of the westerlies during glacial periods may have caused reduced ventilation of deep waters around the perimeter of Antarctica, possibly resulting in an important feedback loop for glacial-interglacial pCO_2 changes (Toggweiler et al., 2006). This may be the kind of circulation shift that will be easier to discern with an accurate and precise map of ε_{Nd} sources, helping to identify possible glacial northward shifts of the ACC major frontal boundaries, for example. Moreover, the evolution of grounded ice delivering large quantities of eroded sediment to the ocean may also be easier to interpret with well-characterised continental ε_{Nd}, shedding light on local-regional glacial dynamics. Although, it will always be challenging to determine the Nd (or other) characteristics of currently subglacial source material. In any case, further constraints on how sediment-water Nd interactions coupled with advection by Southern Ocean currents determine seawater ε_{Nd} distributions, and how these may vary under modern/interglacial and glacial weathering regimes (including the ability to relate measured ε_{Nd} to seawater exposure time, and hence estimate possible deep storage in a highly stratified ocean), can assist in reaching an improved understanding of fundamental climate dynamics on glacial-interglacial timescales.

The important regulating role of the Atlantic Meridional Overturning Circulation (AMOC) on the global climate means that it is the focus of numerous Nd isotope studies aiming to reconstruct changes in Atlantic Ocean water mass mixing during the recent (and more distal) geological past, utilising geological archives (e.g. Howe et al., 2017; Lippold et al., 2016; Piotrowski et al., 2012; Roberts et al., 2010) and through Nd isotope-enabled climate modelling (e.g. Arsouze et al., 2010; Arsouze et al., 2008; Pöppelmeier et al., 2020b; Rempfer et al., 2012). The North Atlantic is thus an important region to characterise well, and in the new ε_{Nd} representation, there are a number of moderate updates (Fig. 5). Namely, continental rock to the north of Baffin Bay in north-western Greenland and further in southern Greenland generally has a more unradiogenic representation of -34, compared to -30 in Jeandel et al. (2007). Continental crust surrounding the south and east of the Hudson Bay remain mostly unchanged. However, rock to the north of the bay overall has a more radiogenic signal than previously estimated, the unradiogenic signal here has been changed from -27 to -23 within continental crust directly in contact with seawater here. Over northern Europe, Iceland now has a more radiogenic signal of +7 compared to 0 in the earlier map, but much of the continental crust in north-western Europe and in addition north-western Africa that is directly in contact with seawater remains largely unchanged.

The discrete ε_{Nd} measurements interpolated to produce the continental map in the north-western Atlantic (shown in detail in Fig. 6c) were mainly the same as used in Jeandel et al. (2007) (not shown here, see Supplementary Fig. S6), with a limited addition of samples added to the north of Baffin Bay and Greenland. However, in producing the novel complementary seafloor map, additional marine detrital samples were collected in this important region (Supplementary Fig. S7c), adding greater spatial representation of observations and thus additional constraints in the Labrador Sea and the North Atlantic Ocean to improve our overall characterisation of the sediment-water interface here. Again, these changes may be important when modelling water mass mixing or interpreting ε_{Nd} data in terms of ocean water provenance, the Labrador and Nordic Seas are known sites of North Atlantic Deep Water formation, thus northern-sourced waters in the Atlantic likely obtain their ε_{Nd} signature from weathering of this continental crust and interaction with seafloor sediment (e.g. Stichel et al., 2020).

A marked increase in observations throughout eastern and southern Europe (particularly the Mediterranean region), and much of the African continent has been achieved (Supplementary Fig. S6), which has directly addressed previous regions of data sparsity in the former compilation by Jeandel et al. (2007). For example, our new compilation includes river sediment measurements taken from the Sanaga Basin in Cameroon bordering the South Atlantic (Weldeab et al., 2011), an area which was previously absent of observations. Nonetheless, notable regions of data sparsity persist in our compilation, and thus there remains some significant uncertainty in our continental ε_{Nd} characterisation in those areas, which include eastern Africa (notably Somalia), Oman, Pakistan, western India and eastern Brazil. It is advised that in these regions, users consider this data limitation and uncertainty in ε_{Nd} when applying/interpreting results.

In summary, our new continental map has incorporated an extensive and up-to-date compilation of published ε_{Nd} observations. It has considerably improved upon the previous version, primarily through a vast increase in the number and spatial coverage of ε_{Nd} observations and directly addressing key regions of data scarcity. This now allows for more accurate and data-constrained interpretations of ε_{Nd} measurements, both in terms of Nd cycling and for use as a water provenance and weathering tracer.

4.3. *Improvements to previously utilised seafloor ε_{Nd} distribution*

Du et al. (2020) noted some inaccuracies of previous model schemes for margin ε_{Nd} boundary conditions that represented a simplified characterisation of seafloor ε_{Nd} distributions produced by linearly extrapolating the data presented by Jeandel et al. (2007). In some locales, this technique did not appropriately capture the distribution suggested by core-top detrital measurements, for example extrapolating observations from southeast Greenland to a wider geographical area yielded extremely unradiogenic ε_{Nd} (-35) in the Irminger Sea where core-top measurements suggested a much more radiogenic signal (-5). Adopting a similar linear extrapolation approach, adding in further constraints by Blanchet (2019), Pöppelmeier et al. (2020b) imposed a global seafloor sediment ε_{Nd} map within a global Nd-isotope enabled model. This was done to explore the possible role of a benthic flux in accurately simulating global marine ε_{Nd} and [Nd], and investigating regionally elevated benthic fluxes in the Northwest Atlantic to test how localised inputs of poorly weathered detrital material could explain the observed early Holocene seawater ε_{Nd} anomaly (Howe et al., 2017; Lippold et al., 2016; Pöppelmeier et al., 2020a; Pöppelmeier et al., 2019). Through inclusion of a benthic flux, Pöppelmeier et al. (2020b) found an improved global modern model-data fit for [Nd] was produced relative to previous schemes, as well as an equivalent level of skill in predicting seawater ε_{Nd} compared to previous studies.

With the addition of over 3,500 extra observations to the initial Nd compilation by Blanchet (2019), including an additional 842 relevant Holocene samples than utilised in this most recent study from Pöppelmeier et al. (2020b), we have vastly increased the number and the spatial coverage of appropriate observations in order to characterise

the ε_{Nd} of the entire sediment-water interface. This particularly includes the addition of more distal seafloor detrital observations, notably covering the eastern North Atlantic, Central Pacific, northern Indian Ocean and the Southern Ocean (Fig. 1). As a result, we have overcome, or at least greatly limited the occurrence of extrapolation biases highlighted in previous model boundary conditions within our new, detailed and constrained seafloor ε_{Nd} maps. Furthermore, in producing a broadly representative global seafloor ε_{Nd} distribution, under the consideration of margin-seafloor continuity and inclusion/application of state-of-the-art knowledge within our methodology (though acknowledging the limitations of persistent data scarcity), we have improved markedly upon earlier work. For example, our seafloor ε_{Nd} representation in the Irminger Sea is -6, which is more consistent with local core-top observations and representative of radiogenic detrital input from the Iceland hotspot. The unradiogenic signal of -23 and -33 associated with Proterozoic and Archean crust respectively in southeastern Greenland, which has previously been extrapolated out to the Irminger Sea, is now constrained to coastal margins. Furthermore, in the seafloor sediment boundary conditions presented by Pöppelmeier et al. (2020b), extrapolation of observations from the Antarctic into the deep South Pacific Ocean give it a very unradiogenic signal of -20, whereas our more radiogenic characterisation of -6 ε_{Nd} is more consistent with detrital observations and with the geology of this area (i.e. proximity to the East Pacific Rise). We were able to achieve this improvement by refining the spatial variability around Antarctica compared to earlier work using a larger compilation (as discussed Section 4.2) and by including additional marine detrital observations in the South Pacific.

The presented seafloor ε_{Nd} maps therefore provide a considerable improvement upon previous simplified linear extrapolation methods. Our key ambition in this regard is to enable users ease of access to appropriate boundary conditions and thus to facilitate future improved model ε_{Nd} representation. By doing so, we hope to have empowered the community to progress our understanding of sediment-water interaction of Nd and further to build upon this established database, incorporating further understanding of the sediment ε_{Nd} distributions and its role in governing the Nd characteristics of seawater.

4.4. Modelling applications and future work

We envisage that one of the major applications of our new ε_{Nd} distributions will be for designing/implementing the boundary conditions required for Nd-isotope models. Such models could range in complexity from relatively simple box-models to full complexity general circulation models. What all have in common, is the need for pre-defined Nd sources. With the emergent (but still debated) benthic flux hypothesis, future models will require knowledge of the ε_{Nd} of seafloor sediment to be able to constrain a benthic flux and model the non-conservative processes involved in marine Nd cycling.

The new datasets presented in this study are therefore useful for further modelling applications like the research undertaken by Pöppelmeier et al. (2020b) in exploring sedimentary Nd sources. For example, they can be used to examine the nature and magnitude/rate of a benthic flux, and to produce quantitative estimates of a global benthic Nd flux into seawater. Our work will facilitate the community to build upon previous modelling efforts (Arsouze et al., 2009; Gu et al., 2019; Pöppelmeier et al., 2020b; Siddall et al., 2008) and explicitly, quantitatively test the range of proposed major sources, sinks and internal cycling mechanisms that govern modern marine Nd distributions. In this way, our new maps, which span the whole ocean-sediment interface, can be employed to examine current paradigms in Nd cycling, including the geographical and geochemical extent of sediment-ocean Nd interactions, and additionally may be used to better estimate Nd ocean residence time. Specifically, it will be more straightforward to systematically explore the sensitivity of ε_{Nd} and [Nd] to different benthic source parameterisations and distributions. This could be achieved, for example, by (i) examining a range of sediment fluxes, (ii) exploring further regional elevated sources from poorly chemically weathered material, and/or (iii) estimating the non-conservative sedimentary processes and the validity of such schemes in producing realistic modern ε_{Nd} and [Nd] distributions. Our new maps additionally enable sensitivity tests in models to explore how physical changes to the strength and structure of ocean circulation impact marine ε_{Nd} and [Nd] under a bottom-up model of marine Nd cycling. Such investigations would undoubtedly provide useful information towards constraining marine Nd budgets, which is essential for robust interpretation and continued application of Nd isotopes as a useful tracer of ocean circulation.

The modern North Pacific represents a key location for testing the benthic flux hypothesis, and thus an important region for modelling applications since the first benthic flux measurements from Abbott et al. (2015b) were taken on the Pacific margin, providing direct evidence for a sedimentary Nd source here. Further, under modern sluggish circulation in the deep Pacific, and alongside detrital input of labile volcanic material into the region, we believe it is an important region to test the potential relabelling of bottom water masses by a benthic flux, and could even be suitable to explore the use of ε_{Nd} as a kinematic tracer. Our seafloor sediment ε_{Nd} distribution presented here now enables more detailed exploration within the Pacific, and thus may enable a new perspective on what could be considered a previously overlooked, but potentially important region for understanding global marine Nd cycling. Further, although not a modern region of deep water formation, the North Pacific may have been a significant contributor to global overturning at times in the past (e.g. Hague et al., 2012; Rae et al., 2014), here conceptual studies could be used to explore changes in ε_{Nd} distributions as a result of enhanced convection and the presence of Pacific Deep Water formation. These could provide a context for how sedimentary controls govern seawater ε_{Nd} under various idealised palaeo reconstructions of circulation states, it must be noted, however, that utilising the global sediment ε_{Nd} maps presented here for such experiments would be limited by the assumption of stable sedimentary Nd fluxes through time (e.g. not accounting for changes in sedimentation rates and/or distribution of detrital sediment). Regardless, such studies would provide an important first step towards quantifying the potential overprinting affect that a benthic flux may have on bottom waters under various circulation regimes.

The seafloor ε_{Nd} maps presented here also create the opportunity to test further hypotheses related to constraining particle-seawater interaction in marine Nd-cycling. Haley et al. (2017) suggested that a large difficulty in resolving the Nd paradox could be a result of undue emphasis placed on reversible scavenging, with the mass transfer required via vertical water column processes being implausible to explain fully the observed [Nd] increases with depth. The sediment ε_{Nd} distributions presented here would enable global sensitivity experiments to utilise these maps, in conjunction with the comprehensive nature of GEOTRACES seawater Nd sampling, to constrain further both water column and sedimentary processes that govern marine Nd.

Further applications could also involve testing the role of a benthic flux on seawater ε_{Nd} in the North Atlantic under different circulation regimes. Under the benthic flux hypothesis the limited expression of non-conservative behaviour in the modern North Atlantic has been attributed not to a lack of sedimentary source, but as a result of a short benthic flux exposure time relative to high ventilation rates (Du et al., 2020; Haley et al., 2017). This behaviour cannot always be assumed, particularly during times when the AMOC was believed to be much weaker in the recent geological past (McManus et al., 2004). As such, idealised studies, for example analysing Atlantic end member ε_{Nd} under a current (high ventilation) and also a reduced AMOC state, would provide valuable information on how benthic flux exposure times may influence seawater ε_{Nd}, useful especially for interpreting palaeoceanographic ε_{Nd} records.

The high-resolution (0.5 °× 0.5°) gridded maps of the continental and seafloor detrital ε_{Nd} are provided in Supplementary Dataset S1 and S2, the maps are also available in vector format, and so can be accessed

at different spatial resolutions to suit specific user applications. These observations thus form the basis of exploring the benthic flux hypothesis in numerical models in order to understand and quantify its potential role in controlling the marine distribution of Nd isotopes, working towards solving the 'Nd paradox'. These data products have been designed to facilitate more modelling and sensitivity studies, with a future aim of coordinating a Nd isotope enabled model intercomparison study.

In closing, appropriate to current understanding of sedimentary Nd sources, we chose to represent the dominant ε_{Nd} signal using lithology and sediment types to inform the origin, age distribution and environment of sediment particles in contact with the ocean, as a first order approach to quantifying the sediment reactive Nd signal. The application of such a method in this work is supported by results from Du et al. (2020), who used a conceptual model to relate the non-conservative ε_{Nd} to published core-top detrital sediment, finding that these two characteristics are well correlated globally. Nonetheless, there still remains uncertainty regarding sediment-water exchange of Nd, especially an incomplete understanding of the controls on dissolved ε_{Nd} distribution in the deep ocean (Wilson et al., 2013), and with particular regard to assessing the main reactive Nd phases in the sediment, which ultimately interact the most with the overlying water column. To narrow down or eliminate these uncertainties, detailed further analyses of global sediment compositions, inputs, transport history, ageing, mineral chemistry, local pore water chemistry and redox state are required (Abbott, 2019; Abbott et al., 2019; Wilson et al., 2013). Such additional research would better inform the work we have undertaken and could be used to refine our proposed ε_{Nd} distributions, assuming there are a sufficient number of available ε_{Nd} measurements from the identified reactive phases. In such a case, it would be useful to perform sensitivity studies on both the regional distribution of ε_{Nd} arrived at by interpolating different selections of sediment types and reactive phases, and on numerically predicted water column ε_{Nd} achieved by utilising those different distributions as model inputs. The compilation and data products presented here do not seek to estimate the reactive sedimentary Nd phases, and we have avoided making complex assumptions about how such phases may behave differently. However, by highlighting this discussion, and visualising the distribution of seafloor ε_{Nd} surmised from currently available data, our work draws attention to current gaps in the observational record and their potential effect on our collective perspective of sedimentary Nd sources to the ocean. Moreover, we hope this will pave the way towards reaching a better understanding of the lability of Nd in deep sea sediment as well as its role in marine Nd cycling and continue the application of ε_{Nd} as a valuable tool for palaeoceanographic reconstruction.

5. Summary and conclusion

The important role of sediment-water interaction in governing oceanic Nd sources and sinks is widely accepted. However, the detail of these processes remain some of the least understood aspects of marine Nd cycling. The updated compilation of published and new sedimentary ε_{Nd} measurements from the continental margins and deep ocean presented here build upon the work of Jeandel et al. (2007), extending the remit of the previous study to include measurements from pore waters and deep seafloor detrital samples in order to improve the characterisation of global ε_{Nd} distributions at the entire sediment-ocean interface. Thus, our new continuous, global, gridded datasets provide the opportunity to explore the non-conservative sedimentary processes that control global Nd cycling. Our results are especially designed for investigating marine Nd cycling, particularly to aid in constraining the magnitude and ε_{Nd} from sediment-water interaction and constrain how this influences the distribution of marine ε_{Nd}. The maps can be used in the implementation of Nd isotopes in numerical models to perform sensitivity and palaeo-experiments, enabling the explicit simulation and quantification of non-conservative sedimentary Nd sources (e.g. testing of a possible benthic flux) and examining the relationship between circulation speed, detrital sediment composition and magnitude of sedimentary inputs under modern and recent (i.e. Quaternary) palaeoceanographic reconstructions. All of this offers a concrete way forward to improve the application of Nd isotopes as a useful tracer of water provenance and mixing, and potentially also as a kinematic tracer of ocean circulation. Future work may aid more rigorous, process-based corrections to evolve this tool. Specifically, once Nd sediment-water interactions within under-studied oceanic regions and sediment types have been more widely analysed, this work will lead to a better understanding of the mechanisms of sediment composition on upward Nd fluxes into seawater.

Data availability

The presented database of ε_{Nd} measurements, along with our global, gridded datasets and all input files for reproducing the maps are available at: https://doi.org/10.5518/928. The ε_{Nd} database will also be made publicly available on the GFZ data repository (https://dataservices.gfz-potsdam.de/panmetaworks/showshort.php?id=escidoc:4094893). Please contact Cécile Blanchet (blanchet@gfz-potsdam.de) for additional data. In addition to the ε_{Nd} data, the input files include the Continental Geological Base Map, as used by Jeandel et al. (2007), which was an earlier version obtained from http://pyroxene.ens.fr/spiplabocnrs/spip.php?rubrique67; GlobSed: Global Sediment Thickness Map (currently also available from http://earthdynamics.org/data/GlobSed); and the Seafloor Lithology Map (currently available from ftp://ftp.earthbyte.org/papers/Dutkiewicz_etal_seafloor_lithology/).

Author contributions

SMR designed and executed the main project, including preparing the manuscript, with core guidance from RFI and TF, and further input from all co-authors. Additionally, CB curated the ε_{Nd} database, KT provided a compilation of detrital Nd data, CC and EM contributed new Southern Ocean Nd data, and TW compiled the large Southern Ocean published Nd dataset. CJ and TA provided support concerning their previous methodology, including input files.

Declaration of Competing Interest

The authors declare that they have no known competing financial interests or personal relationships that could have appeared to influence the work reported in this paper.

Acknowledgements

SMR was funded by the Natural Environment Research Council (NERC) SPHERES Doctoral Training Partnership (grant number: NE/L002574/1). We thank April Abbott, Jianghui Du and Andy Ridgwell for informative discussions while undertaking the work. We are grateful to two anonymous reviewers for prompt and helpful comments that improved the manuscript, and to Karen H. Johannesson for swift editorial handling.

Appendix A. Supplementary data

Supplementary data to this article can be found online at https://doi.org/10.1016/j.chemgeo.2021.120119.

References

Abbott, A.N., 2019. A benthic flux from calcareous sediments results in non-conservative neodymium behavior during lateral transport: A study from the Tasman Sea. Geology 47, 363–366. https://doi.org/10.1130/g45904.1.

Abbott, A.N., Haley, B.A., McManus, J., 2015a. Bottoms up: Sedimentary control of the deep North Pacific Ocean's εNd signature. Geology 43, 1035–1038. https://doi.org/10.1130/G37114.1.

Abbott, A.N., Haley, B.A., McManus, J., Reimers, C.E., 2015b. The sedimentary flux of dissolved rare earth elements to the ocean. Geochim. Cosmochim. Acta 154, 186–200. https://doi.org/10.1016/j.gca.2015.01.010.

Abbott, A.N., Haley, B.A., McManus, J., 2016. The impact of sedimentary coatings on the diagenetic Nd flux. Earth Planet. Sci. Lett. 449, 217–227. https://doi.org/10.1016/j.epsl.2016.06.001.

Abbott, A.N., Löhr, S., Trethewy, M., 2019. Are clay minerals the primary control on the oceanic rare earth element budget? Front. Mar. Sci. 6, 1–19. https://doi.org/10.3389/fmars.2019.00504.

Arsouze, T., Dutay, J.-C.C., Lacan, F., Jeandel, C., 2007. Modeling the neodymium isotopic composition with a global ocean circulation model. Chem. Geol. 239, 165–177. https://doi.org/10.1016/j.chemgeo.2006.12.006.

Arsouze, T., Dutay, J.C., Kageyama, M., Lacan, F., Alkama, R., Marti, O., Jeandel, C., 2008. A modeling sensitivity study of the influence of the Atlantic meridional overturning circulation on neodymium isotopic composition at the last glacial maximum. Clim. Past 4, 191–203. https://doi.org/10.5194/cp-4-191-2008.

Arsouze, T., Dutay, J.C., Lacan, F., Jeandel, C., 2009. Reconstructing the Nd oceanic cycle using a coupled dynamical- biogeochemical model. Biogeosciences 6, 2829–2846. https://doi.org/10.5194/bg-6-2829-2009.

Arsouze, T., Treguier, A.M., Peronne, S., Dutay, J.C., Lacan, F., Jeandel, C., 2010. Modeling the Nd isotopic composition in the North Atlantic basin using an eddy-permitting model. Ocean Sci. 6, 789–797. https://doi.org/10.5194/os-6-789-2010.

Asahara, Y., Takeuchi, F., Nagashima, K., Harada, N., Yamamoto, K., Oguri, K., Tadai, O., 2012. Provenance of terrigenous detritus of the surface sediments in the Bering and Chukchi Seas as derived from Sr and Nd isotopes: Implications for recent climate change in the Arctic regions. Deep. Res. Part II Top. Stud. Oceanogr. 61–64, 155–171. https://doi.org/10.1016/j.dsr2.2011.12.004.

Ayache, M., Dutay, J.C., Arsouze, T., Révillon, S., Beuvier, J., Jeandel, C., 2016. High-resolution neodymium characterization along the Mediterranean margins and modelling of Nd distribution in the Mediterranean basins. Biogeosciences 13, 5259–5276. https://doi.org/10.5194/bg-13-5259-2016.

Bacon, M.P., Anderson, R.F., 1982. Distribution of thorium isotopes between dissolved and particulate forms in the deep sea. J. Geophys. Res. 87, 2045–2056. https://doi.org/10.1029/JC087iC03p02045.

Basak, C., Pahnke, K., Frank, M., Lamy, F., Gersonde, R., 2015. Neodymium isotopic characterization of Ross Sea Bottom Water and its advection through the southern South Pacific. Earth Planet. Sci. Lett. 419, 211–221. https://doi.org/10.1016/j.epsl.2015.03.011.

Basile, I., Grousset, F.E., Revel, M., Petit, J.R., Biscaye, P.E., Barkov, N.I., 1997. Patagonian origin of glacial dust deposited in East Antarctica (Vostok and Dome C) during glacial stages 2, 4 and 6. Earth Planet. Sci. Lett. 146, 573–589. https://doi.org/10.1016/s0012-821x(96)00255-5.

Bayon, G., German, C.R., Boella, R.M., Milton, J.A., Taylor, R.N., Nesbitt, R.W., 2002. An improved method for extracting marine sediment fractions and its application to Sr and Nd isotopic analysis. Chem. Geol. 187, 179–199. https://doi.org/10.1016/S0009-2541(01)00416-8.

Bayon, G., Toucanne, S., Skonieczny, C., André, L., Bermell, S., Cheron, S., Dennielou, B., Etoubleau, J., Freslon, N., Gauchery, T., Germain, Y., Jorry, S.J., Ménot, G., Monin, L., Ponzevera, E., Rouget, M.L., Tachikawa, K., Barrat, J.A., 2015. Rare earth elements and neodymium isotopes in world river sediments revisited. Geochim. Cosmochim. Acta 170, 17–38. https://doi.org/10.1016/j.gca.2015.08.001.

Bertram, C.J., Elderfield, H., 1993. The geochemical balance of the rare earth elements and neodymium isotopes in the oceans. Geochim. Cosmochim. Acta 57, 1957–1986. https://doi.org/10.1016/0016-7037(93)90087-D.

Blanchet, C.L., 2019. A database of marine and terrestrial radiogenic Nd and Sr isotopes for tracing earth-surface processes. Earth Syst. Sci. Data 11, 741–759. https://doi.org/10.5194/essd-11-741-2019.

Blaser, P., Lippold, J., Gutjahr, M., Frank, N., Link, J.M., Frank, M., 2016. Extracting foraminiferal seawater Nd isotope signatures from bulk deep sea sediment by chemical leaching. Chem. Geol. 439, 189–204. https://doi.org/10.1016/j.chemgeo.2016.06.024.

Blaser, P., Pöppelmeier, F., Schulz, H., Gutjahr, M., Frank, M., Lippold, J., Heinrich, H., Link, J.M., Hoffmann, J., Szidat, S., Frank, N., 2019. The resilience and sensitivity of Northeast Atlantic deep water εNd to overprinting by detrital fluxes over the past 30,000 years. Geochim. Cosmochim. Acta 245, 79–97. https://doi.org/10.1016/j.gca.2018.10.018.

Bryce, J.G., DePaolo, D.J., Lassiter, J.C., 2005. Geochemical structure of the Hawaiian plume: Sr, Nd, and Os isotopes in the 2.8 km HSDP-2 section of Mauna Kea volcano. Geochem. Geophys. Geosyst. 6. https://doi.org/10.1029/2004GC000809.

Chase, Z., Anderson, R.F., Fleisher, M.Q., Kubik, P.W., 2002. The influence of particle composition and particle flux on scavenging of Th, Pa and Be in the ocean. Earth Planet. Sci. Lett. 204, 215–229. https://doi.org/10.1016/S0012-821X(02)00984-6.

Cook, C.P., van de Flierdt, T., Williams, T., Hemming, S.R., Iwai, M., Kobayashi, M., Jimenez-Espejo, F.J., Escutia, C., González, J.J., Khim, B.K., McKay, R.M., Passchier, S., Bohaty, S.M., Riesselman, C.R., Tauxe, L., Sugisaki, S., Galindo, A.L., Patterson, M.O., Sangiorgi, F., Pierce, E.L., Brinkhuis, H., Klaus, A., Fehr, A., Bendle, J.A.P., Bijl, P.K., Carr, S.A., Dunbar, R.B., Flores, J.A., Hayden, T.G., Katsuki, K., Kong, G.S., Nakai, M., Olney, M.P., Pekar, S.F., Pross, J., Röhl, U., Sakai, T., Shrivastava, P.K., Stickley, C.E., Tuo, S., Welsh, K., Yamane, M., 2013. Dynamic behaviour of the East Antarctic ice sheet during Pliocene warmth. Nat. Geosci. 6, 765–769. https://doi.org/10.1038/ngeo1889.

Crocket, K.C., Hill, E., Abell, R.E., Johnson, C., Gary, S.F., Brand, T., Hathorne, E.C., 2018. Rare earth element distribution in the ne Atlantic: evidence for benthic sources, longevity of the seawater signal, and biogeochemical cycling. Front. Mar. Sci. 5 https://doi.org/10.3389/fmars.2018.00147.

Dausmann, V., Frank, M., Gutjahr, M., Rickli, J., 2017. Glacial reduction of AMOC strength and long-term transition in weathering inputs into the Southern Ocean since the mid-Miocene: evidence from radiogenic Nd and Hf isotopes. Paleoceanography 32, 265–283. https://doi.org/10.1002/2016PA003056.

Du, J., Haley, B.A., Mix, A.C., 2016. Neodymium isotopes in authigenic phases, bottom waters and detrital sediments in the Gulf of Alaska and their implications for paleocirculation reconstruction. Geochim. Cosmochim. Acta 193, 14–35. https://doi.org/10.1016/j.gca.2016.08.005.

Du, J., Haley, B.A., Mix, A.C., 2020. Evolution of the Global Overturning Circulation since the Last Glacial Maximum based on marine authigenic neodymium isotopes. Quat. Sci. Rev. 241, 106396 https://doi.org/10.1016/j.quascirev.2020.106396.

Dutkiewicz, A., Müller, R.D., O'Callaghan, S., Jónasson, H., 2015. Census of seafloor sediments in the world's ocean. Geology 43, 795–798. https://doi.org/10.1130/G36883.1.

Ehlert, C., Frank, M., Haley, B.A., Böniger, U., De Deckker, P., Gingele, F.X., 2011. Current transport versus continental inputs in the eastern Indian Ocean: radiogenic isotope signatures of clay size sediments. Geochem. Geophys. Geosyst. 12. https://doi.org/10.1029/2011GC003544.

Fielding, L., Najman, Y., Millar, I., Butterworth, P., Ando, S., Padoan, M., Barfod, D., Kneller, B., 2017. A detrital record of the Nile River and its catchment. J. Geol. Soc. London. 174, 301–317. https://doi.org/10.1144/jgs2016-075.

van de Flierdt, T., Hemming, S.R., Goldstein, S.L., Gehrels, G.E., Cox, S.E., 2008. Evidence against a young volcanic origin of the Gamburtsev Subglacial Mountains, Antarctica. Geophys. Res. Lett. 35, L21303. doi:https://doi.org/10.1029/2008GL035564.

van de Flierdt, T., Pahnke, K., Amakawa, H., Andersson, P., Basak, C., Coles, B., Colin, C., Crocket, K., Frank, M., Frank, N., Goldstein, S.L., Goswami, V., Haley, B.A., Hathorne, E.C., Hemming, S.R., Henderson, G.M., Jeandel, C., Jones, K., Kreissig, K., Lacan, F., Lambelet, M., Martin, E.E., Newkirk, D.R., Obata, H., Pena, L., Piotrowski, A.M., Pradoux, C., Scher, H.D., Schöberg, H., Singh, S.K., Stiche, T., Tazoe, H., Vance, D., Yang, J., 2012. GEOTRACES intercalibration of neodymium isotopes and rare earth element concentrations in seawater and suspended particles. Part 1: Reproducibility of results for the international intercomparison. Limnol. Oceanogr. Methods 10, 234–251. https://doi.org/10.4319/lom.2012.10.234.

van de Flierdt, T., Griffths, A.M., Lambelet, M., Little, S.H., Stichel, T., Wilson, D.J., 2016. Neodymium in the oceans: A global database, a regional comparison and implications for palaeoceanographic research. Philos. Trans. R. Soc. A Math. Phys. Eng. Sci. doi:https://doi.org/10.1098/rsta.2015.0293.

Gischler, E., 2006. Sedimentation on Rasdhoo and Ari Atolls, Maldives, Indian ocean. Facies 52, 341–360. https://doi.org/10.1007/s10347-005-0031-3.

Goldstein, S.L., Hemming, S.R., 2003. Long-lived isotopic tracers in oceanography, paleoceanography, and ice-sheet dynamics. Treatise on Geochemistry 453–483. https://doi.org/10.1016/B0-08-043751-6/06179-X.

Goldstein, O'Nions, Hamilton, et al., 1984. A Sm-Nd isotopic study of atmospheric dusts and particulates from major river systems. Earth and Planetary Science Letters 70, 221–236. https://doi.org/10.1016/0012-821X(84)90007-4.

Gorsline, D.S., 1984. A review of fine-grained sediment origins, characteristics. transport and deposition. Geol. Soc. Spec. Publ. 15, 17–34. https://doi.org/10.1144/GSL.SP.1984.015.01.02.

Grasse, P., Stichel, T., Stumpf, R., Stramma, L., Frank, M., 2012. The distribution of neodymium isotopes and concentrations in the Eastern Equatorial Pacific: water mass advection versus particle exchange. Earth Planet. Sci. Lett. 353–354, 198–207. https://doi.org/10.1016/j.epsl.2012.07.044.

Grenier, M., Jeandel, C., Lacan, F., Vance, D., Venchiarutti, C., Cros, A., Cravatte, S., 2013. From the subtropics to the central equatorial Pacific Ocean: neodymium isotopic composition and rare earth element concentration variations. J. Geophys. Res. Ocean. 118, 592–618. https://doi.org/10.1029/2012JC008239.

Grousset, F.E., Biscaye, P.E., Zindler, A., Prospero, J., Chester, R., 1988. Neodymium isotopes as tracers in marine sediments and aerosols: North Atlantic. Earth Planet. Sci. Lett. 87, 367–378. https://doi.org/10.1016/0012-821X(88)90001-5.

Grousset, F.E., Biscaye, P.E., Revel, M., Petit, J.R., Pye, K., Joussaume, S., Jouzel, J., 1992. Antarctic (Dome C) ice-core dust at 18 k.y. B.P.: Isotopic constraints on origins. Earth Planet. Sci. Lett. 111, 175–182. https://doi.org/10.1016/0012-821X(92)90177-W.

Grousset, F.E., Parra, M., Bory, A., Martinez, P., Bertrand, P., Shimmield-M, G., Ellamn, R.M., 1998. Saharan Wind Regimes Traced by the Sr-Nd Isotopic Composition of Subtropical Atlanti Sediments: Last Glacial Maximum vs Today, Quaternary Science Reviews. https://doi.org/10.1016/S0277-3791(97)00048-6.

Gu, S., Liu, Z., Jahn, A., Rempfer, J., Zhang, J., Joos, F., 2019. Modeling neodymium isotopes in the ocean component of the community earth system model (CESM1). J. Adv. Model. Earth Syst. 11, 624–640. https://doi.org/10.1029/2018MS001538.

Hague, A.M., Thomas, D.J., Huber, M., Korty, R., Woodard, S.C., Jones, L.B., 2012. Convection of North Pacific deep water during the early Cenozoic. Geology 40, 527–530. https://doi.org/10.1130/G32886.1.

Haley, B.A., Polyak, L., 2013. Pre-modern Arctic Ocean circulation from surface sediment neodymium isotopes. Geophys. Res. Lett. 40, 893–897. https://doi.org/10.1002/grl.50188.

Haley, B.A., Du, J., Abbott, A.N., McManus, J., 2017. The impact of benthic processes on rare earth element and neodymium isotope distributions in the oceans. Front. Mar. Sci. 4, 426. https://doi.org/10.3389/fmars.2017.00426.

Hall, R., 2002. Cenozoic geological and plate tectonic evolution of SE Asia and the SW Pacific: Computer-based reconstructions, model and animations. J. Asian Earth Sci. 20, 353–431. https://doi.org/10.1016/S1367-9120(01)00069-4.

Han, Y., Zhao, T., Song, L., Fang, X., Yin, Y., Deng, Z., Wang, S., Fan, S., 2011. A linkage between Asian dust, dissolved iron and marine export production in the deep ocean. Atmos. Environ. 45, 4291–4298. https://doi.org/10.1016/j.atmosenv.2011.04.078.

Hemming, S.R., Van De Flierdt, T., Goldstein, S.L., Franzese, A.M., Roy, M., Gastineau, G., Landrot, G., 2007. Strontium isotope tracing of terrigenous sediment dispersal in the Antarctic circumpolar current: Implications for constraining frontal positions. Geochem. Geophys. Geosyst. 8. https://doi.org/10.1029/2006GC001441.
Henderson, G.M., Heinze, C., Anderson, R.F., Winguth, A.M.E., 1999. Global distribution of the 230Th flux to ocean sediments constrained by GCM modelling. Deep. Res. Part I Oceanogr. Res. Pap. 46, 1861–1893. https://doi.org/10.1016/S0967-0637(99)00030-8.
Horikawa, K., Asahara, Y., Yamamoto, K., Okazaki, Y., 2010. Intermediate water formation in the Bering Sea during glacial periods: Evidence from neodymium isotope ratios. Geology 38, 435–438. https://doi.org/10.1130/G30225.1.
Howe, J.N.W., Piotrowski, A.M., Noble, T.L., Mulitza, S., Chiessi, C.M., Bayon, G., 2016. North atlantic deep water production during the last glacial maximum. Nat. Commun. 7 https://doi.org/10.1038/ncomms11765.
Howe, J.N.W., Piotrowski, A.M., Hu, R., Bory, A., 2017. Reconstruction of east–west deep water exchange in the low latitude Atlantic Ocean over the past 25,000 years. Earth Planet. Sci. Lett. 458, 327–336. https://doi.org/10.1016/j.epsl.2016.10.048.
Hu, R., Piotrowski, A.M., 2018. Neodymium isotope evidence for glacial-interglacial variability of deepwater transit time in the Pacific Ocean. Nat. Commun. 9 https://doi.org/10.1038/s41467-018-07079-z.
Huck, C.E., Van De Flierdt, T., Jiménez-Espejo, F.J., Bohaty, S.M., Röhl, U., Hammond, S. J., 2016. Robustness of fossil fish teeth for seawater neodymium isotope reconstructions under variable redox conditions in an ancient shallow marine setting. Geochemistry, Geophys Geosystems 17, 679–698. https://doi.org/10.1002/2015GC006218.
Innocent, C., Fagel, N., Stevenson, R.K., Hillaire-Marcel, C., 1997. Sm-Nd signature of modern and late Quaternary sediments from the northwest North Atlantic: Implications for deep current changes since the Last Glacial Maximum. Earth Planet. Sci. Lett. 146, 607–625. https://doi.org/10.1016/s0012-821x(96)00251-8.
Jacobsen, S.B., Wasserburg, G.J., 1980. Sm-Nd evolution of chondrites. Earth Planet. Sci. Lett. 50, 139–155. https://doi.org/10.1016/0012-821X(80)90125-9.
Jahnke, R.A., Emerson, S.R., Reimers, C.E., Schuffert, J., Ruttenberg, K., Archer, D., 1989. Benthic recycling of biogenic debris in the eastern tropical Atlantic Ocean. Geochim. Cosmochim. Acta 53, 2947–2960. https://doi.org/10.1016/0016-7037(89)90171-3.
Jeandel, C., 2016. Overview of the mechanisms that could explain the "Boundary Exchange" at the land-ocean contact. Philos. Trans. R. Soc. A Math. Phys. Eng. Sci. https://doi.org/10.1098/rsta.2015.0287.
Jeandel, C., Oelkers, E.H., 2015. The influence of terrigenous particulate material dissolution on ocean chemistry and global element cycles. Chem. Geol. https://doi.org/10.1016/j.chemgeo.2014.12.001.
Jeandel, C., Bishop, J.K., Zindler, A., 1995. Exchange of neodymium and its isotopes between seawater and small and large particles in the Sargasso Sea. Geochim. Cosmochim. Acta 59, 535–547. https://doi.org/10.1016/0016-7037(94)00367-U.
Jeandel, C., Arsouze, T., Lacan, F., Téchiné, P., Dutay, J.C., 2007. Isotopic Nd compositions and concentrations of the lithogenic inputs into the ocean: a compilation, with an emphasis on the margins. Chem. Geol. 239, 156–164. https://doi.org/10.1016/j.chemgeo.2006.11.013.
Jeandel, C., Delattre, H., Grenier, M., Pradoux, C., Lacan, F., 2013. Rare earth element concentrations and Nd isotopes in the Southeast Pacific Ocean. Geochemistry, Geophys Geosystems 14, 328–341. https://doi.org/10.1029/2012GC004309.
Jones, C.E., Halliday, A.N., Rea, D.K., Owen, R.M., 1994. Neodymium isotopic variations in North Pacific modern silicate sediment and the insignificance of detrital REE contributions to seawater. Earth Planet. Sci. Lett. 127, 55–66. https://doi.org/10.1016/0012-821X(94)90197-X.
Jones, K.M., Khatiwala, S.P., Goldstein, S.L., Hemming, S.R., van de Flierdt, T., 2008. Modeling the distribution of Nd isotopes in the oceans using an ocean general circulation model. Earth Planet. Sci. Lett. 272, 610–619. https://doi.org/10.1016/j.epsl.2008.05.027.
Jonkers, L., Zahn, R., Thomas, A., Henderson, G., Abouchami, W., François, R., Masque, P., Hall, I.R., Bickert, T., 2015. Deep circulation changes in the central South Atlantic during the past 145 kyrs reflected in a combined231Pa/230Th, Neodymium isotope and benthic δC13 record. Earth Planet. Sci. Lett. 419, 14–21. https://doi.org/10.1016/j.epsl.2015.03.004.
Khélifi, N., Sarnthein, M., Frank, M., Andersen, N., Garbe-Schönberg, D., 2014. Late Pliocene variations of the Mediterranean outflow. Mar. Geol. 357, 182–194. https://doi.org/10.1016/j.margeo.2014.07.006.
Lacan, F., Jeandel, C., 2005. Acquisition of the neodymium isotopic composition of the North Atlantic Deep Water. Geochemistry, Geophys. Geosystems 6. https://doi.org/10.1029/2005GC000956.
Lacan, F., Tachikawa, K., Jeandel, C., 2012. Neodymium isotopic composition of the oceans: a compilation of seawater data. Chem. Geol. 300–301, 177–184. https://doi.org/10.1016/j.chemgeo.2012.01.019.
Lambelet, M., van de Flierdt, T., Butler, E.C.V., Bowie, A.R., Rintoul, S.R., Watson, R.J., Remenyi, T., Lannuzel, D., Warner, M., Robinson, L.F., Bostock, H.C., Bradtmiller, L. I., 2018. The neodymium isotope fingerprint of adélie coast bottom water. Geophys. Res. Lett. 45, 11,247–11,256. https://doi.org/10.1029/2018GL080074.
Lippold, J., Gutjahr, M., Blaser, P., Christner, E., de Carvalho Ferreira, M.L., Mulitza, S., Christl, M., Wombacher, F., Böhm, E., Antz, B., Cartapanis, O., Vogel, H., Jaccard, S. L., 2016. Deep water provenance and dynamics of the (de)glacial Atlantic meridional overturning circulation. Earth Planet. Sci. Lett. 445, 68–78. https://doi.org/10.1016/j.epsl.2016.04.013.
Lupker, M., France-Lanord, C., Galy, V., Lavé, J.Ô., Kudrass, H., 2013. Increasing chemical weathering in the Himalayan system since the Last Glacial Maximum. Earth Planet. Sci. Lett. 365, 243–252. https://doi.org/10.1016/j.epsl.2013.01.038.
Lynch-Stieglitz, J., Marchitto, T.M., 2003. Tracers of past ocean circulation. In: Treatise on Geochemistry, Second edition, pp. 435–452. https://doi.org/10.1016/B978-0-08-095975-7.00616-1.
Maccali, J., Hillaire-Marcel, C., Carignan, J., Reisberg, L.C., 2013. Geochemical signatures of sediments documenting Arctic sea-ice and water mass export through Fram Strait since the Last Glacial Maximum. Quat. Sci. Rev. 64, 136–151. https://doi.org/10.1016/j.quascirev.2012.10.029.
Martin, E.E., Scher, H., 2006. A Nd isotopic study of southern sourced waters and indonesian throughflow at intermediate depths in the Cenozoic Indian Ocean. Geochemistry, Geophys. Geosystems 7. https://doi.org/10.1029/2006GC001302.
McManus, J.F., Francois, R., Gherardl, J.M., Kelgwin, L., Drown-Leger, S., 2004. Collapse and rapid resumption of Atlantic meridional circulation linked to deglacial climate changes. Nature 428, 834–837. https://doi.org/10.1038/nature02494.
Mikhalsky, E.V., Laiba, A.A., Beliatsky, B.V., 2006. Tectonic subdivision of the prince charles mountains: a review of geologic and isotopic data. Antarctica 69–81. https://doi.org/10.1007/3-540-32934-x_9.
Mikhalsky, E.V., Sheraton, J.W., Kudriavtsev, I.V., Sergeev, S.A., Kovach, V.P., Kamenev, I.A., Laiba, A.A., 2013. The mesoproterozoic Rayner Province in the Lambert Glacier area: its age, origin, isotopic structure and implications for Australia-Antarctica correlations. Geol. Soc. Spec. Publ. 383, 35–57. https://doi.org/10.1144/SP383.1.
Nakai, S., Halliday, A.N., Rea, D.K., 1993. Provenance of dust in the Pacific Ocean. Earth Planet. Sci. Lett. 119, 143–157. https://doi.org/10.1016/0012-821X(93)90012-X.
Newkirk, D.R., Martin, E.E., 2009. Circulation through the Central American Seaway during the Miocene carbonate crash. Geology 37, 87–90. https://doi.org/10.1130/G25193A.1.
Pearce, C.R., Jones, M.T., Oelkers, E.H., Pradoux, C., Jeandel, C., 2013. The effect of particulate dissolution on the neodymium (Nd) isotope and Rare Earth Element (REE) composition of seawater. Earth Planet. Sci. Lett. 369–370, 138–147. https://doi.org/10.1016/j.epsl.2013.03.023.
Peucker-Ehrenbrink, B., Miller, M.W., Arsouze, T., Jeandel, C., 2010. Continental bedrock and riverine fluxes of strontium and neodymium isotopes to the oceans. Geochemistry, Geophys. Geosystems 11. https://doi.org/10.1029/2009GC002869.
Pierce, E.L., Williams, T., van de Flierdt, T., Hemming, S.R., Goldstein, S.L., Brachfeld, S. A., 2011. Characterizing the sediment provenance of East Antarctica's weak underbelly: the Aurora and Wilkes sub-glacial basins. Paleoceanography 26. https://doi.org/10.1029/2011PA002127.
Piotrowski, A.M., Galy, A., Nicholl, J.A.L., Roberts, N., Wilson, D.J., Clegg, J.A., Yu, J., 2012. Reconstructing deglacial North and South Atlantic deep water sourcing using foraminiferal Nd isotopes. Earth Planet. Sci. Lett. 357–358, 289–297. https://doi.org/10.1016/j.epsl.2012.09.036.
Pöppelmeier, F., Blaser, P., Gutjahr, M., Süfke, F., Thornalley, D.J.R., Grützner, J., Jakob, K.A., Link, J.M., Szidat, S., Lippold, J., 2019. Influence of ocean circulation and benthic exchange on deep northwest atlantic nd isotope records during the past 30,000 years. Geochemistry, Geophys Geosystems 20, 4457–4469. https://doi.org/10.1029/2019GC008271.
Pöppelmeier, F., Blaser, P., Gutjahr, M., Jaccard, S.L., Frank, M., Max, L., Lippold, J., 2020a. Northern sourced water dominated the atlantic ocean during the last glacial maximum. Geology 48. https://doi.org/10.1130/G47628.1.
Pöppelmeier, F., Scheen, J., Blaser, P., Lippold, J., Gutjahr, M., Stocker, T.F., 2020b. Influence of elevated Nd fluxes on the northern Nd isotope end member of the Atlantic during the early Holocene. Paleoceanogr. Paleoclimatology. https://doi.org/10.1029/2020pa003973.
Porcelli, D., Andersson, P.S., Baskaran, M., Frank, M., Björk, G., Semiletov, I., 2009. The distribution of neodymium isotopes in Arctic Ocean basins. Geochim. Cosmochim. Acta 73, 2645–2659. https://doi.org/10.1016/j.gca.2008.11.046.
Rae, J.W.B., Sarnthein, M., Foster, G.L., Ridgwell, A., Grootes, P.M., Elliott, T., 2014. Deep water formation in the North Pacific and deglacial CO2 rise. Paleoceanography 29, 645–667. https://doi.org/10.1002/2013PA002570.
Rahlf, P., Hathorne, E., Laukert, G., Gutjahr, M., Weldeab, S., Frank, M., 2020. Tracing water mass mixing and continental inputs in the southeastern Atlantic Ocean with dissolved neodymium isotopes. Earth Planet. Sci. Lett. 530, 115944 https://doi.org/10.1016/j.epsl.2019.115944.
Rempfer, J., Stocker, T.F., Joos, F., Dutay, J.-C., Siddall, M., 2011. Modelling Nd-isotopes with a coarse resolution ocean circulation model: Sensitivities to model parameters and source/sink distributions. Geochim. Cosmochim. Acta 75, 5927–5950. https://doi.org/10.1016/j.gca.2011.07.044.
Rempfer, J., Stocker, T.F., Joos, F., Dutay, J.C., 2012. On the relationship between Nd isotopic composition and ocean overturning circulation in idealized freshwater discharge events. Paleoceanography 27, PA3211. https://doi.org/10.1029/2012PA002312.
Revel, M., Cremer, M., Grousset, F.E., Labeyrie, L., 1996. Grain-size and Sr-Nd isotopes as tracer of paleo-bottom current strength. Northeast Atlantic Ocean, Marine Geology. https://doi.org/10.1016/0025-3227(96)00005-9.
Roberts, N.L., Piotrowski, A.M., 2015. Radiogenic Nd isotope labeling of the northern NE Atlantic during MIS 2. Earth Planet. Sci. Lett. 423, 125–133. https://doi.org/10.1016/j.epsl.2015.05.011.
Roberts, N.L., Piotrowski, A.M., McManus, J.F., Keigwin, L.D., 2010. Synchronous deglacial overturning and water mass source changes. Science (80-.) 327, 75–78. https://doi.org/10.1126/science.1178068.
Rousseau, T.C.C., Sonke, J.E., Chmeleff, J., Van Beek, P., Souhaut, M., Boaventura, G., Seyler, P., Jeandel, C., 2015. Rapid neodymium release to marine waters from lithogenic sediments in the Amazon estuary. Nat. Commun. 6 https://doi.org/10.1038/ncomms8592.
Roy, M., van de Flierdt, T., Hemming, S.R., Goldstein, S.L., 2007. 40Ar/39Ar ages of hornblende grains and bulk Sm/Nd isotopes of circum-Antarctic glacio-marine

sediments: implications for sediment provenance in the southern ocean. Chem. Geol. 244, 507–519. https://doi.org/10.1016/j.chemgeo.2007.07.017.
Scher, H.D., Martin, E.E., 2006. Timing and climatic consequences of the opening of drake passage. Science (80-.). 312, 428–430. doi:https://doi.org/10.1126/science.1120044.
Scheuvens, D., Schütz, L., Kandler, K., Ebert, M., Weinbruch, S., 2013. Bulk composition of northern African dust and its source sediments - a compilation. Earth-Science Rev. https://doi.org/10.1016/j.earscirev.2012.08.005.
Sepulchre, P., Arsouze, T., Donnadieu, Y., Dutay, J.C., Jaramillo, C., Le Bras, J., Martin, E., Montes, C., Waite, A.J., 2014. Consequences of shoaling of the Central American Seaway determined from modeling Nd isotopes. Paleoceanography 29, 176–189. https://doi.org/10.1002/2013PA002501.
Siddall, M., Henderson, G.M., Edwards, N.R., Frank, M., Müller, S.A., Stocker, T.F., Joos, F., 2005. 231Pa/230Th fractionation by ocean transport, biogenic particle flux and particle type. Earth Planet. Sci. Lett. 237, 135–155. https://doi.org/10.1016/j.epsl.2005.05.031.
Siddall, M., Stocker, T.F., Henderson, G.M., Joos, F., Frank, M., Edwards, N.R., Ritz, S.P., Müller, S.A., 2007. Modeling the relationship between 231Pa/230Th distribution in North Atlantic sediment and Atlantic meridional overturning circulation. Paleoceanography 22. https://doi.org/10.1029/2006PA001358.
Siddall, M., Khatiwala, S., van de Flierdt, T., Jones, K., Goldstein, S.L., Hemming, S., Anderson, R.F., 2008. Towards explaining the Nd paradox using reversible scavenging in an ocean general circulation model. Earth Planet. Sci. Lett. 274, 448–461. https://doi.org/10.1016/j.epsl.2008.07.044.
Sigman, D.M., Jaccard, S.L., Haug, G.H., 2004. Polar ocean stratification in a cold climate. Nature 428, 59–63. https://doi.org/10.1038/nature02357.
Simões Pereira, P., van de Flierdt, T., Hemming, S.R., Hammond, S.J., Kuhn, G., Brachfeld, S., Doherty, C., Hillenbrand, C.D., 2018. Geochemical fingerprints of glacially eroded bedrock from West Antarctica: Detrital thermochronology, radiogenic isotope systematics and trace element geochemistry in Late Holocene glacial-marine sediments. Earth Sci. Rev. 182, 204–232. https://doi.org/10.1016/j.earscirev.2018.04.011.
Stephens, B.B., Keeling, R.F., 2000. The influence of antarctic sea ice on glacial-interglacial CO2 variations. Nature 404, 171–174. https://doi.org/10.1038/35004556.
Stichel, T., Kretschmer, S., Geibert, W., Lambelet, M., Plancherel, Y., Rutgers van der Loeff, M., van de Flierdt, T., 2020. Particle–seawater interaction of neodymium in the North Atlantic. ACS Earth Sp. Chem. doi:https://doi.org/10.1021/acsearthspacechem.0c00034.
Straume, E.O., Gaina, C., Medvedev, S., Hochmuth, K., Gohl, K., Whittaker, J.M., Abdul Fattah, R., Doornenbal, J.C., Hopper, J.R., 2019. GlobSed: updated total sediment thickness in the world's oceans. Geochemistry, Geophys. Geosystems 20, 1756–1772. https://doi.org/10.1029/2018GC008115.
Stumpf, R., Frank, M., Schönfeld, J., Haley, B.A., 2010. Late Quaternary variability of Mediterranean Outflow Water from radiogenic Nd and Pb isotopes. Quat. Sci. Rev. 29, 2462–2472. https://doi.org/10.1016/j.quascirev.2010.06.021.
Stumpf, R., Kraft, S., Frank, M., Haley, B., Holbourn, A., Kuhnt, W., 2015. Persistently strong Indonesian Throughflow during marine isotope stage 3: Evidence from radiogenic isotopes. Quat. Sci. Rev. 112, 197–206. https://doi.org/10.1016/j.quascirev.2015.01.029.
Tachikawa, K., Jeandel, C., Vangriesheim, A., Dupré, B., 1999. Distribution of rare earth elements and neodymium isotopes in suspended particles of the tropical Atlantic Ocean (EUMELI site). Deep. Res. Part I Oceanogr. Res. Pap. 46, 733–755. https://doi.org/10.1016/S0967-0637(98)00089-2.
Tachikawa, K., Athias, V., Jeandel, C., 2003. Neodymium budget in the modern ocean and paleo-oceanographic implications. J. Geophys. Res. 108, 3254. https://doi.org/10.1029/1999JC000285.
Tachikawa, K., Roy-Barman, M., Michard, A., Thouron, D., Yeghicheyan, D., Jeandel, C., 2004. Neodymium isotopes in the Mediterranean Sea: Comparison between seawater and sediment signals. Geochim. Cosmochim. Acta 68, 3095–3106. https://doi.org/10.1016/j.gca.2004.01.024.
Tachikawa, K., Arsouze, T., Bayon, G., Bory, A., Colin, C., Dutay, J.C., Frank, N., Giraud, X., Gourlan, A.T., Jeandel, C., Lacan, F., Meynadier, L., Montagna, P., Piotrowski, A.M., Plancherel, Y., Pucéat, E., Roy-Barman, M., Waelbroeck, C., 2017. The large-scale evolution of neodymium isotopic composition in the global modern and Holocene ocean revealed from seawater and archive data. Chem. Geol. 457, 131–148. https://doi.org/10.1016/j.chemgeo.2017.03.018.
Taylor, McLennan, McCulloch, et al., 1983. Geochemistry of loess, continental crustal composition and crustal model ages. Geochimica et Cosmochimica Acta 47, 1897–1905. https://doi.org/10.1016/0016-7037(83)90206-5.
Toggweiler, J.R., Russell, J.L., Carson, S.R., 2006. Midlatitude westerlies, atmospheric CO2, and climate change during the ice ages. Paleoceanography 21. https://doi.org/10.1029/2005PA001154.
Toucanne, S., Soulet, G., Freslon, N., Silva Jacinto, R., Dennielou, B., Zaragosi, S., Eynaud, F., Bourillet, J.F., Bayon, G., 2015. Millennial-scale fluctuations of the European Ice Sheet at the end of the last glacial, and their potential impact on global climate. Quat. Sci. Rev. 123, 113–133. https://doi.org/10.1016/j.quascirev.2015.06.010.
Voelker, A.H.L., Lebreiro, S.M., Schönfeld, J., Cacho, I., Erlenkeuser, H., Abrantes, F., 2006. Mediterranean outflow strengthening during northern hemisphere coolings: A salt source for the glacial Atlantic? Earth Planet. Sci. Lett. 245, 39–55. https://doi.org/10.1016/j.epsl.2006.03.014.
Vogt-Vincent, N., Lippold, J., Kaboth-Bahr, S., Blaser, P., 2020. Ice-rafted debris as a source of non-conservative behaviour for the εNd palaeotracer: insights from a simple model. Geo-Marine Lett. https://doi.org/10.1007/s00367-020-00643-x.
Walter, H.J., Hegner, E., Diekmann, B., Kuhn, G., Rutgers Van Der Loeff, M.M., 2000. Provenance and transport of terrigenous sediment in the South Atlantic Ocean and their relations to glacial and interglacial cycles: Nd and Sr isotopic evidence. Geochim. Cosmochim. Acta 64, 3813–3827. https://doi.org/10.1016/S0016-7037(00)00476-2.
Weldeab, S., Frank, M., Stichel, T., Haley, B., Sangen, M., 2011. Spatio-temporal evolution of the West African monsoon during the last deglaciation. Geophys. Res. Lett. 38 https://doi.org/10.1029/2011GL047805.
Wilson, D.J., Piotrowski, A.M., Galy, A., Clegg, J.A., 2013. Reactivity of neodymium carriers in deep sea sediments: Implications for boundary exchange and paleoceanography. Geochim. Cosmochim. Acta 109, 197–221. https://doi.org/10.1016/j.gca.2013.01.042.
Wilson, D.J., Crocket, K.C., van de Flierdt, T., Robinson, L.F., Adkins, J.F., 2015. Dynamic intermediate ocean circulation in the North Atlantic during Heinrich Stadial 1: A radiocarbon and neodymium isotope perspective. Paleoceanography 29, 1072–1093. https://doi.org/10.1002/2014PA002674.
Xie, R.C., Marcantonio, F., Schmidt, M.W., 2014. Reconstruction of intermediate water circulation in the tropical North Atlantic during the past 22,000 years. Geochim. Cosmochim. Acta 140, 455–467. https://doi.org/10.1016/j.gca.2014.05.041.
Zhang, Z., Jiang, F., Li, T., Yang, D., Zhou, X., Xiong, Z., Qiu, X., Jia, Q., Yan, Y., Feng, X., 2020. Sea-level changes controlled detrital sediment inputs to the Bicol Shelf in the western Philippine Sea since 150 ka. J. Oceanol. Limnol. 38, 1153–1168. https://doi.org/10.1007/s00343-020-0051-4.
Zheng, X.Y., Plancherel, Y., Saito, M.A., Scott, P.M., Henderson, G.M., 2016. Rare earth elements (REEs) in the tropical South Atlantic and quantitative deconvolution of their non-conservative behavior. Geochim. Cosmochim. Acta 177, 217–237. https://doi.org/10.1016/j.gca.2016.01.018.